UNIVERSITY OF NOVI SAD
FACULTY OF SCIENCES
DEPARTMENT OF MATHEMATICS AND INFORMATICS

Isidora Rapajić

Modelling Capillary Rise In The Vascular Tissue Of Plants

- Master's Thesis-

Mentor:

Prof. Srboljub Simić, Ph.D.

2021, Novi Sad

Acknowledgements

I would like to express my gratitude and appreciation to Prof. Srboljub Simić for his guidance at all stages of this research, continuous assistance during my Master's studies and inspirational lectures on Continuum Mechanics.

I am grateful to the board, Prof. Danijela Rajter Ćirić, Prof. Mirjana Štrboja and Prof. Milan Borišev, for reviewing this thesis and providing valuable advice.

Special thanks to European Consortium for Mathematics in Industry (ECMI) for organising Virtual Modelling Week in 2020 and instructor Mateusz Świtała for introducing this topic and raising interesting questions that motivated this work.

I wish to extend my thanks to Aleksandar for reading this text and giving me strong support, both academic and emotional, throughout the studies.

Finally, I wish to express my deepest gratitude and appreciation to my parents Biljana and Milan and grandparents Paraskeva, Dragan, Nada and Nedeljko for unending care and support in every aspect of my life.

Contents

Preface

Water is crucial for the life and growth of plants. The process of photosynthesis requires water to be continuously absorbed and lost.

Some plants have developed specialized vascular tissue (xylem) which provides a physical mechanism for supplying water to photosynthetic organs. The two major processes in water transport are molecular diffusion and mass flow. Diffusion is the gradual mixing of molecules and eventual dissipation of concentration differences, and it is usually caused by thermal motion of molecules. Mass flow, on the other hand, is fluid movement caused by pressure gradient whenever there is a suitable pathway. Pressure gradient ocurrs due to transpiration, which is an important factor for the global water cycle. [1] Pressure-driven mass flow is the main mechanism of water transport through xylem.

The first attempts to describe vascular system of plants and to find analogy with blood circulation started with William Harvey (1628) and Marcello Malpighi (1661). It was suggested that the role of tracheids and vessels, which are the building blocks of xylem, is air transport and that fibres should exist for transport of water and minerals. Transport tissue was identified in the 18th and early 19th century. There were debates about whether conducting elements of xylem are filled with water, air or air bubbles interspersed with water. A significant breakthrough was made in 1891 by Eduard Strasburger who made a review of existing knowledge in plant hydraulics in his book *"On construction and function of the conduits in plants"*. The first experimental demonstration was made by Joseph Boehm in 1892 and the cohesion-tension theory (CTT) was proposed in 1894 by John Joly and Henry Horatio Dixon.

CTT is a theory that provides an explanation of water uptake in plants and especially in trees. It is based on the assumption that "high tensions" exist in plants ($-3\,\mathrm{MPa}$ in crop plants, $-4\,\mathrm{MPa}$ in trees, $-10\,\mathrm{MPa}$ in desert species). [2; 17; 25]. Moreover, the risk of cavitation is a controversial aspect of the CTT. However, it is shown that properties of water can prevent cavitation to a certain extent. [5].

The goal of this thesis is to formulate and analyse mathematical model for capillary uptake of water in the xylem.

A biological explanation of the phenomena with exact terminology is provided in Chapter 1.

The equation for capillary flow was derived from Newton's second law and proven experimentally by Edward Washburn in 1921. [32] Chapter 2 of this thesis is dedicated to derivation of Washburn's equation from first principles, i.e. mass and momentum balance equations. Derivation can be split in two stages. In the first stage we make assumptions about velocity field and pressure field that follow directly from Navier-Stokes equations in local form. Pressure field is shown to depend only on $z-$coordinate while velocity field is modeled by Poiseuille flow. In the second stage, Washburn's

[1] 39 % of transpired water returns as rain. [26]

equation is derived from integral form of Navier-Stokes equations in cylindrical coordinates. Finally, the scaled Washburn's equation is derived, which contain only one dimensionless parameter.

Analysis of a solution is presented in Chapter 3 of this thesis. Existence and uniqueness are proved using Banach's fixed point theorem. Bounds on a solution are also provided using the energy estimate, and domain and range are determined with respect to initial water column height.

Chapter 4 contains rigorous asymptotic analysis which reveals several possible regimes of the flow. They are obtained by neglecting certain physical mechanisms in the model. Furthermore, asymptotic behavior of the system is determined by means of linear stability analysis. Monotonic and oscillatory behaviour of a solution are distinguished in the neighborhood of the stationary point. Different behaviour is also demonstrated by phase portraits and numerical solution of the governing equation. Model is validated using experimental data for short-time limit.

Motivation for this study came from the project realised during First Virtual ECMI Modeling Week 2020 [20]. In particular, ideas about modeling of water uptake were taken as a starting point in this study. Also, analysis of simplified models, which was explained in [20] on phenomenological basis, in this thesis was put on firm theoretical ground.

Chapter 1

Water Transport in Plants

In this Chapter, a brief introduction to plant physiology with a focus on vascular tissue and water transport is presented in Section 1.1. The Cohesion–Tension Theory is explained in Section 1.2.

1.1 Vascular Tissue

Water is essential in the life of a plant. Dehydratation can cause malfunctioning of cellular processes, since plant cells are composed of water. Moreover, the structure and properties of proteins, membranes, nucleid acids and other cell constituents are highly dependent on water. Therefore, plants must balance their uptake and loss of water.

Water potential Ψ_w is a measure of the free energy of water per unit volume [Jm^{-3}] and represents a good overall indicator of plant health. Cell growth, photosyntesis and crop productivity are strongly influenced by water potential and all its components. The major factors influencing the water potential in plants are concentration Ψ_s, pressure Ψ_p and gravity Ψ_g.

$$\Psi_w = \Psi_s + \Psi_p + \Psi_g.$$

When we consider water transport at the cell level, the gravitational component Ψ_g is omitted since it is negligible compared to the osmotic potential and hydrostatic pressure. For soils that have large concentration of salts Ψ_s is significant, otherwise it is negligible. The hydrostatic pressure Ψ_p is very close to zero for wet soils. As a soil dries out, Ψ_p decreases and becomes negative. Absorbing water from soil, plants establish a pressure gradient. Water enters the plant through the root system and proceeds flowing to the stem.

The process of water evaporating from leaf surface is called **transpiration** and it causes water to move upwards. The focus of our work is analysis of water uptake through the stem. It occurs in response to pressure difference, whenever there is a suitable pathway.

In most plants, **a vascular tissue (xylem)** provides water flow through stem. It is the longest part of the pathway of water transport, with a low resistance. **Tracheids and vessels** are building blocks of xylem. The conducting cells of tracheids and vessels have specialised anatomy, that provide transport of water with high efficiency. Those are "dead" cells, which means that they have neither membranes nor organelles. Both tracheids and vessels vary within and between species. Tracheids are elongated and hollow cells, which are present in all vascular plants. Neighbouring tracheids are

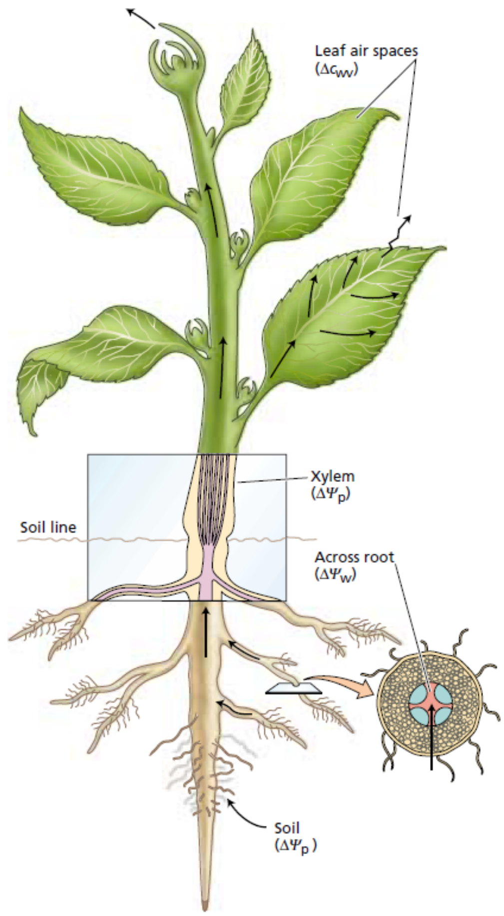

Figure 1.1. Main driving forces for water flow through the plant. Δc_{wv} - differences in water vapor concentration, Ψ_p - hydrostatic pressure, $\Delta\Psi_w$ - water potential [30]

connected by **pits** on their walls, forming **pit pairs**. Pit pairs form a low-resisting path for water flow between tracheids. **The pit membrane** represents the porous layer between pit pairs.

Vessel elements are shorter and wider comparing to tracheids and have developed **perforation plates**, a place where they connect to one another. In that way, vessel elements build **vessels**. Like tracheids, vessels are dead cells that provide a low-resistance pathway for water movement

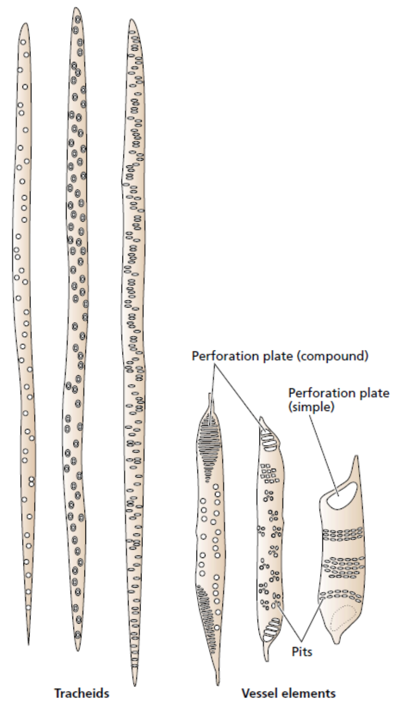

Figure 1.2. Tracheids and vessel elements. [30]

1.2 The Cohesion-Tension Theory

Water, as a solvent, is the medium for the movement of molecules. Moreover, it directly participates in many essential chemical reactions. These properties are the consequence of the polar structure of the water molecule.

In the water molecule, oxygen atom is covalently bonded to two hydrogen atoms. An angle of 105° is formed between two O—H bonds. The electrons of the covalent bond are attracted to the oxygen atom (because of the higher electronegativity). A partial negative charge appears at the oxygen part of the molecule, while partial positive charges appear at each hydrogen. Since these partial charges are equal, the water molecule carries no total charge.

Hydrogen bonds are weak electrostatic attractions between water molecules. Many physical properties of water are the consequence of it. Hydrogen bonds can be formed between water and the other molecules with electronegative atoms (e.g. ionic substances, some sugars and proteins). Molecules that are on the free surface of water are more strongly connected to neighbouring water molecules than to gas molecules. This results in tendency of free surface to minimise its surface area. **Surface tension** is the energy required for the surface area of a free surface to be increased. Apart from influencing the shape of the surface, the surface tension may create a pressure in the rest of the liquid. **Cohesion** is the attraction between water molecules, which is a consequence of hydrogen bonding. **Adhesion** represents attraction of water to a solid phase (e.g. a cell wall or a glass surface). **Capillarity** is the movement of water along the capillary tube, which is a result of

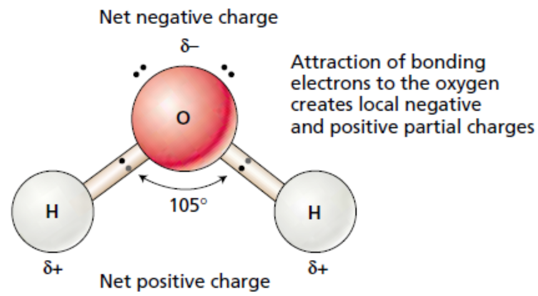

Figure 1.3. Diagram of the water molecule [30]

cohesion, adhesion and surface tension.

The Cohesion-Tension theory (CTT) is based on mechanisms of liquid transport and on the anatomical properties of the xylem. First proposed toward the end of the nineteenth century, it has been verified by a large number of experiments [6; 31]. However, it has been a controversial subject for more than a century. The main controversy surrounds the question of whether water columns in the xylem can sustain the large tensions necessary to pull water up tall trees. Moreover, the risk of cavitation has been widely discussed. Cavitation is forming of a gas bubble, which breaks the continuity of a water column and block water transport in the xylem. It usually occurs as a consequence of the extreme weather (e.g. freezing).

The CTT theory can be sumarised in the following statements [29]:

1. A continuous network of liquid columns is formed within the plant. It spreads from the root to the evaporating surface (leaves). Most of the transport network is composed of vessels and tracheids.

2. The vascular pathway has hydraulic continuity, which means that the variations or tensions are transfered continuously throughout the plant.

3. The evaporating surface (from leaves) generates surface tension, which is a driving force for the water movement.

4. Evaporation generates a curvature in the water menisci, which is sufficiently small to support water columns as long as one hundred meters.

5. Evaporation lowers the water potential in the xylem elements.

6. Evaporation produces gradients of pressure along the pathway in the plant. Consequently, water from the soil inflows the transpiring surface.

7. Water in the xylem is in the state of tension, due to transpiration (pulling from leaves). In this state, the appearance of a vapor phase within the liquid phase (cavitation) may occur. Even when transpiration stops (e.g. in periods with high relative humidity), water will continue to uptake as long as there exists difference of water potential across the water column.

8. Cohesion and adhesion prevent cavitation to a certain extent.

Note that assumption of CTT is that high tensions could exist in a plant. However, the validity of CTT is not dependent on a specific range of xylem tensions.

The focus of this thesis is water transport through xylem. We will propose a mathematical model for water uptake in a tracheid, which will be approximated by a narrow pipe with no resistance. Moreover, we shall assume that cavitation does not occur during the transport process.

Chapter 2

Mathematical Model of Capillary Rise

This thesis is concerned with modelling and mathematical analysis of the motion of water through the stem. As it is usual in modelling, we tend to develop the model which is simple enough to be feasible for analysis, but also to be rich enough to incorporate the fundamental features of the process.

The process we are concerned about is usually modelled by the motion of a fluid through the vertical cylindrical pipe. Capillary effects are the main driving agent, but also the influence of gravity and viscosity cannot be neglected. Widely accepted model for accurate description of capillary motion of the fluid through the vertical pipe is the Washburn's equation [32]. It is often derived in a simplistic way, starting from the Newton's Law of Motion and applying it to an infinitesimal volume of a fluid in a cylinder [14].

Our aim in this Chapter is to derive the Washburn's equation from the first principles, i.e. from the fundamental equations of continuum mechanics. To that end, we shall firstly review the basic equations of continuum mechanics, needed for our analysis. After that, they will be applied to our specific problem of motion of the fluid in a vertical pipe.

Figure 2.1. Vertical pipes with different diemeters. Heights and shape of the meniscus are different.

In our model, the pipe considered is infinitely long and narrow. The assumption of flat meniscus will be justified in Section 2.2.3. It can be seen in Figure 2.1 how radius of a pipe influences height of a liquid column and shape of a meniscus.

2.1 Foundations of Continuum Mechanics

Basic equations of continuum mechanics generalize the basic laws of mechanics of a material point (particle). Material point is a geometric point in Eucledian space ($\mathbb{R}^3$) to which certain physical properties are attributed. It possesses mass $m \geq 0$, which is constant throughout the motion:

$$m = \text{const.}$$

Position of the particle is determined by a **position vector** $\boldsymbol{x}(t) \in \mathbb{R}^3$, where $t \in \mathbb{R}^+ \cup \{0\}$ is the time. Rate of change of the position vector is the **velocity** $\mathbf{v}(t)$, and rate of change of the velocity is the **acceleration** $\boldsymbol{a}(t)$:

$$\mathbf{v}(t) = \frac{d\boldsymbol{x}(t)}{dt}, \quad \boldsymbol{a}(t) = \frac{d\mathbf{v}(t)}{dt} = \frac{d^2\boldsymbol{x}(t)}{dt^2}.$$

State of motion of the particle is determined by the **momentum** $\boldsymbol{K}(t)$, defined as:

$$\boldsymbol{K}(t) := m\mathbf{v}(t).$$

Newton's Law of Motion postulates that the rate of change of momentum is equal to the force $\boldsymbol{F}$ which acts upon the particle:

$$\frac{d\boldsymbol{K}}{dt} = \boldsymbol{F} \quad \Rightarrow \quad m\boldsymbol{a} = \boldsymbol{F}.$$

In general, force may depend on time, position and velocity of the particle, but does not depend on acceleration:

$$\boldsymbol{F} = \boldsymbol{F}(t, \boldsymbol{x}, \mathbf{v}).$$

In the sequel, we shall define the basic notions of continuum mechanics, and present the fundamental laws that we shall apply [13].

2.1.1 Kinematics of continuum

The basic property of a body in continuum mechanics is that it may occupy regions of Euclidean space $\mathcal{E}$. We may identify the body with the region $\mathcal{B}$ of $\mathcal{E}$ in some fixed configuration, called a **reference configuration**; but the choice of reference configuration is arbitrary.

Hence we consider a body identified with the region $\mathcal{B}$ it occupies in a fixed reference configuration, and refer to $\mathcal{B}$ as the **reference body** and to a point $\boldsymbol{X}$ in $\mathcal{B}$ as a **material point** or **particle**.

Definition 2.1.1. A motion of B is a smooth function $\mathcal{X}$, that assigns to each material point $\boldsymbol{X}$ and time t a point

$$\boldsymbol{x} = \mathcal{X}(\boldsymbol{X}, t),$$

where $\boldsymbol{x}$ is a spatial point occupied by $\boldsymbol{X}$ at time $t \in \mathbb{R}$.

For a fixed t, the function $\mathcal{X}(\boldsymbol{X}, t)$ is called a deformation. Since it depends only on $\boldsymbol{X}$, we introduce a simplified notation:

$$\mathcal{X}_t(\boldsymbol{X}) = \mathcal{X}(\boldsymbol{X}, t).$$

A basic hypothesis is that $\mathcal{X}_t(\boldsymbol{X})$ is one-to-one in $\boldsymbol{X}$, meaning that no two material points can occupy the same spatial point at a given time.

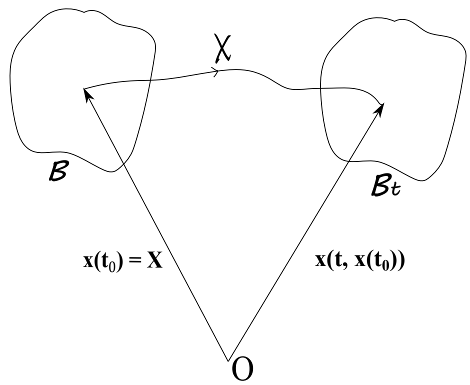

Figure 2.2. Deformation $\mathcal{X}$ which maps reference configuration $\mathcal{B}$ to current configuration $\mathcal{B}_t$.

The region of space occupied by the body at time t, $\mathcal{B}_t = \mathcal{X}_t(B)$, is reffered to as the deformed body at time t. The current configuration, $\mathcal{B}_t$ is the set of points $\boldsymbol{x}$, such that $\boldsymbol{x} = \mathcal{X}(\boldsymbol{X}, t)$ for some $\boldsymbol{X}$ in B. Current configuration is observed during a motion. On the other hand, reference configuration serves to label material points.

The spatial vectors

$$\dot{\mathcal{X}}(\boldsymbol{X}, t) = \frac{\partial \mathcal{X}(\boldsymbol{X}, t)}{\partial t}, \quad \ddot{\mathcal{X}}(\boldsymbol{X}, t) = \frac{\partial^2 \mathcal{X}(\boldsymbol{X}, t)}{\partial t^2}$$

are velocity and acceleration of the material point $\boldsymbol{X}$ at time t.

Since the mapping $\boldsymbol{x} = \mathcal{X}(\boldsymbol{X}, t)$ is one-to-one in $\boldsymbol{X}$ for fixed t it has an inverse

$$\boldsymbol{X} = \mathcal{X}^{-1}(\boldsymbol{x}, t),$$

at each t, the fixed-time inverse is a mapping of the deformed body $\mathcal{B}(t)$ onto the reference body $\mathcal{B}(t_0)$ with the following property

$$\boldsymbol{x} = \mathcal{X}(\boldsymbol{X}, t) \iff \boldsymbol{X} = \mathcal{X}^{-1}(\boldsymbol{x}, t).$$

We refer to $\mathcal{X}^{-1}$ as the reference map. Using the reference map, we can describe the velocity $\dot{\mathcal{X}}$ as a function $\mathbf{v}(\boldsymbol{x}, t)$:

$$\mathbf{v}(\boldsymbol{x}, t) = \dot{\mathcal{X}}(\mathcal{X}^{-1}(\boldsymbol{x}, t), t) \iff \dot{\mathcal{X}}(\boldsymbol{X}, t) = \mathbf{v}(\mathcal{X}(\boldsymbol{X}, t), t).$$

The field $\mathbf{v}$ is material velocity, and $\mathbf{v}(\boldsymbol{x}, t)$ is the velocity of the material point that the spatial point $\boldsymbol{x}$ occupies at time t.

2.1.2 Reynolds' transport theorem

In order to generalise concept of material velocity, let φ denote a scalar, vector or tensor field defined on the body, for all t. We consider φ to be a function $\varphi(\boldsymbol{X}, t)$ of the material point $\boldsymbol{X}$ at time t - this is called the material description of φ. On the other hand, we can consider φ to be a function of the spatial point $\boldsymbol{x}$ and t, i.e. $\phi(\boldsymbol{x}, t)$. This is called a spatial description and it is related to material description through

$$\phi(\boldsymbol{x}, t) = \varphi(\mathcal{X}^{-1}(\boldsymbol{x}, t), t).$$

Similarly, the material description is given by

$$\varphi(\boldsymbol{X}, t) = \phi(\mathcal{X}(\boldsymbol{X}, t), t).$$

The tensor field

$$\boldsymbol{F} = \nabla \mathcal{X}, \quad F_{ij} = \left[\frac{\partial x_i}{\partial X_j} \right]^3_{i,j=1,2,3}$$

is referred to as the **deformation gradient**.

The volumetric Jacobian is of the mapping $\mathcal{X}_t$ is defined as:

$$J = \det \boldsymbol{F} > 0.$$

Note that when transforming volume and surface integrals from the deformed body to the reference body, we replace the volume element dV by JdV_R. In the sequel we shall need the following Lemma, the proof of which may be found in [13].

Lemma 2.1.1. *The volumetric Jacobian is of the mapping $\mathcal{X}_t$ has the following property:*

$$\dot{J} = J \operatorname{div} \mathbf{v}. \tag{2.1}$$

Now we can state and prove Reynolds' transport theorem.

Theorem 2.1.2. *Let ϕ be a smooth spatial field, and assume that ϕ is either scalar valued or vector valued. Then for every part $\mathcal{B}$ and time t,*

$$\frac{d}{dt} \int_{\mathcal{B}(t)} \phi dV = \int_{\mathcal{B}(t)} \left(\dot{\phi} + \phi \operatorname{div} \mathbf{v} \right) dV \tag{2.2}$$

Proof.

$$\begin{aligned} \frac{d}{dt} \int_{\mathcal{B}(t)} \phi(\boldsymbol{x}, t) dV &= \frac{d}{dt} \int_{\mathcal{B}(t_0)} \phi(\boldsymbol{x}(\boldsymbol{X}, t), t) J dV_R = \int_{\mathcal{B}(t_0)} \left(\dot{\phi} J + \phi \dot{J} \right) dV_R \\ &= \int_{\mathcal{B}(t_0)} \left(\dot{\phi} + \phi \operatorname{div} \mathbf{v} \right) J dV_R = \int_{\mathcal{B}(t)} \left(\dot{\phi} + \phi \operatorname{div} \mathbf{v} \right) dV. \end{aligned}$$

□

Reynold's transport theorem provides a mean to evaluate the time rate of change of any physical quantity within material body, provided it is described by its density (a quantity per unit volume).

2.1.3 Mass Balance

One of the most important properties of bodies is that they possess mass. We here consider bodies whose mass is distributed continuously and determined by the mass density.

Global form

Let $\mathcal{P}_t = \mathcal{X}_t(P)$ for some material region $\mathcal{P}$. We write $\rho_R(\boldsymbol{X}) > 0$ for the mass density at the material point $\boldsymbol{X}$ in the reference body $\mathcal{B}$, so that

$$\int_{\mathcal{P}} \rho_R(\boldsymbol{X}) dV_R(\boldsymbol{X})$$

represents the mass of the material region $\mathcal{P}$. We refer to $\rho_R(\boldsymbol{X})$ as the reference mass density.

We write $\rho(\boldsymbol{x}, t) > 0$ for the mass density at the spatial point $\boldsymbol{x}$ in the deformed body $\mathcal{B}_t$, so that the mass of material region $\mathcal{P}_t$ in spatial configuration is

$$\int_{\mathcal{P}_t} \rho(\boldsymbol{x}, t) dV(\boldsymbol{x}).$$

Balance of mass is the requirement that, given any motion

$$\int_{\mathcal{P}} \rho_R(\boldsymbol{X}) dV_R(\boldsymbol{X}) = \int_{\mathcal{P}_t} \rho(\boldsymbol{x}, t) dV(\boldsymbol{x}) \tag{2.3}$$

for every material region $\mathcal{P}$. The left-hand side of (2.3) is independent of time. If we differentiate (2.3) with respect to t, it follows that

$$\frac{d}{dt} \int_{\mathcal{P}_t} \rho(\boldsymbol{x}, t) dV(\boldsymbol{x}) = 0. \tag{2.4}$$

Since (2.3) holds for any material region, it will also hold for body that has a constant mass, M:

$$\int_{\mathcal{B}} \rho_R(\boldsymbol{X}) dV_R(\boldsymbol{X}) = \int_{\mathcal{B}_t} \rho(\boldsymbol{x}, t) dV(\boldsymbol{x}) = M = const. \tag{2.5}$$

Local form

From Reynolds' transport theorem (2.2) and the property of mass balance (2.4), it follows that

$$\int_{\mathcal{P}(t)} (\dot{\rho} + \rho \operatorname{div} \mathbf{v}) \, dV = 0, \quad \forall \mathcal{P}(t) \subset \forall \mathcal{B}(t) \tag{2.6}$$

Since (2.6) holds for any material region $\mathcal{P}(t)$, it implies the local (differential form) of the mass balance

$$\dot{\rho} + \rho \operatorname{div} \mathbf{v} = 0, \quad \forall x \in \mathcal{B}(t). \tag{2.7}$$

The following consequence of the mass balance law can be shown for a spatial scalar field φ:

$$\frac{\partial}{\partial t} (\rho\varphi) + \operatorname{div}(\rho\varphi\mathbf{v}) = \rho\dot{\varphi}. \tag{2.8}$$

2.1.4 Momentum balance

Motions are accompanied by forces. Forces in continuum mechanics are described by

- contact forces between spatial regions that intersect along their boundaries,
- contact forces applied on the boundary of the body by its environment,
- body forces applied on the interior points of a body by environment.

Contact forces and body forces may be measured per unit area and volume in the reference body or per unit volume and area in the deformed body.

To describe the contact forces, Cauchy introduced a surface-traction field $\boldsymbol{t}$, representing the force per unit area of the surface of contact $\mathcal{S}$. It was postulated that surface-traction field at point $\boldsymbol{x} \in \mathcal{S}$ does not depend on the shape of the surface in the neighbourhood of the point, but only on its orientation through the unit normal vector $\boldsymbol{n}$, i.e $\boldsymbol{t}(\boldsymbol{n}(\boldsymbol{x},t),\boldsymbol{x},t)$, defined for each unit vector $\boldsymbol{n}$, each $\boldsymbol{x}$ in $\mathcal{B}_t$ and each t.

Let $\mathcal{P}$ and $\mathcal{D}$ be adjacent spatial regions, and $\mathcal{S}$ surface of contact,

$$\mathcal{S} = P \cap \mathcal{D}.$$

To determine the total contact force $\boldsymbol{F}_s$ acting upon surface $\mathcal{S}$, we integrate traction over $\mathcal{S}$:

$$\boldsymbol{F}_s := \int_{\mathcal{S}} \boldsymbol{t}(\boldsymbol{n}(\boldsymbol{x},t),\boldsymbol{x},t)dA(\boldsymbol{x}) \equiv \int_{\mathcal{S}} \boldsymbol{t}(\boldsymbol{n})dA, \tag{2.9}$$

where $dA(\boldsymbol{x})$ is the surface element of $\mathcal{S}$, and the second integral will be used in the sequel as a shorthand. If the total contact force is to be computed for the boundary of the spatial region $\mathcal{P}$, we have

$$\boldsymbol{F}_s = \int_{\partial\mathcal{P}_t} \boldsymbol{t}(\boldsymbol{n})dA. \tag{2.10}$$

The environment can also exert forces on interior point of $\mathcal{B}_t$, with a classical example of such a force being that due to gravity. Such forces are determined by a vector field $\boldsymbol{b}(\boldsymbol{x},t)$ expressing the force per unit volume $\boldsymbol{F}_v$ exerted by the environment on $\boldsymbol{x}$. The total body force which acts upon spatial region $\mathcal{P}_t$ is defined as

$$\boldsymbol{F}_v := \int_{\mathcal{P}_t} \boldsymbol{b}dV. \tag{2.11}$$

Global form

Given a spatial region $\mathcal{P}_t$ the integral

$$\boldsymbol{K}(t) = \int_{P_t} \rho(\boldsymbol{x},t)\mathbf{v}(\boldsymbol{x},t)dV$$

represents the **linear momentum** of $\mathcal{P}_t$.

The fundamental law of motion is the **balance law for linear momentum** given by

$$\frac{d\boldsymbol{K}}{dt} = \boldsymbol{F}.$$

Since the net force $\boldsymbol{F}$ can be expressed as a sum of a contact force and a body force,

$$\boldsymbol{F} = \boldsymbol{F}_s + \boldsymbol{F}_v,$$

it follows that

$$\frac{d}{dt}\int_{\mathcal{P}_t} \rho(\boldsymbol{x},t)\mathbf{v}(\boldsymbol{x},t)dV = \int_{\partial\mathcal{P}_t} \boldsymbol{t}(\boldsymbol{n})dA + \int_{\mathcal{P}_t} \boldsymbol{b}dV, \tag{2.12}$$

which is linear momentum balance law in integral (global) form written for any spatial region $\mathcal{P}_t \subset \mathcal{B}_t$ of the body in spatial configuration.

Cauchy theorem

A deep result, central to continuum mechanics is existence of Cauchy stress as a consequence of balance of forces.

Theorem 2.1.3 (Existence of stress)**.** *A consequence of the momentum balance law* (2.12) *is that there exists a spatial tensor field* $\boldsymbol{T}(\boldsymbol{x},t)$*, called the Cauchy stress, such that for each unit vecor* $\boldsymbol{n}$*, it holds that*

$$\boldsymbol{t}(\boldsymbol{n},\boldsymbol{x},t) = \boldsymbol{T}(\boldsymbol{x},t)\boldsymbol{n}. \tag{2.13}$$

The proof of the Theorem is omitted and may be found in [12; 13]. Another important property of the Cauchy stress is that it is symmetric

$$\boldsymbol{T} = \boldsymbol{T}^T,$$

which is a consequence of the angular momentum balance law [13].

Local form

In view of Cauchy's theorem, we can rewrite the linear momentum balance law (2.12) as

$$\int_{\mathcal{P}_t} (\rho\dot{\mathbf{v}} - \operatorname{div}\boldsymbol{T} - \boldsymbol{b})\, dV = \mathbf{0}.$$

Since it must be satisfied for all spatial regions $\mathcal{P}_t \subset \mathcal{B}_t$, the local momentum balance law follows

$$\rho\dot{\mathbf{v}} = -\operatorname{div}\boldsymbol{T} + \boldsymbol{b}. \tag{2.14}$$

2.1.5 Constitutive equations

The balance laws are presumed to hold for all bodies: solid, liquid or gas. On the other hand, particular materials are defined by additional assumptions in the form of **constitutive equations**, which describe the response of the material. It is necessary to introduce constitutive relations for two reasons: first, to describe the material whose motion is under consideration; second, to close the system of equations that represent our model, since in general balance laws the number of unknown fields is larger than the number of equations.

Newtonian fluids

In this thesis we shall be concerned with a motion of water, which belongs to a special class of materials known as **Newtonian** or **viscous fluids**. Therefore, we shall give a brief review of the basic constitutive realtions for fluids. A fluid is **compressible** if it holds that

$$dV \neq J dV_R.$$

In contrast, if the fluid is **incompressible**, it follows that $dV = dV_R$ From (2.1) it follows that

$$J = 1 \implies \dot{J} = 0.$$

Therefore, from (2.1)

$$\operatorname{div} \mathbf{v} = 0.$$

Local form of mass balance (2.7) implies that

$$\dot{\rho} = 0 \implies \rho = const. \tag{2.15}$$

A **perfect (Euler) fluid** is a fluid whose stress tensor is expressed by the constitutive equation

$$\boldsymbol{T} = -p\boldsymbol{I}, \quad p > 0,$$

where the positive scalar p is called **pressure**.

The model of perfect (Euler) fluid is the simplest model of fluids used in continuum mechanics. It is in good agreement with real situations under a variety of conditions. However, fluids may exhibit more complex behaviours that have to be described in a proper way. To do that we have to rely on a certain set of fundamenal constitutive statements. The restricted form of basic constitutive statement is as follows [3]:

The stress at the point $\boldsymbol{x}$ at time t is uniquely determined by fields derived from the motion of $\mathcal{B}$ and also evaluated at $(\boldsymbol{x}, t)$.

In order to define constitutive relation for stress in case of Newtonian incompressible fluids, we introduce the folowing spatial tensor fields

- **Velocity gradient - L** $:= \operatorname{grad} \mathbf{v} = \nabla \mathbf{v}$
- **Stretching - D** $:= \frac{1}{2}\left(\mathbf{L} + \mathbf{L}^T\right) = \frac{1}{2}\left(\nabla \mathbf{v} + (\nabla \mathbf{v})^T\right)$

The constitutive equation for viscous fluids is

$$\boldsymbol{t} = -p(\rho)\mathbf{I} + \boldsymbol{f}(\rho, \mathbf{L}),$$

where $\boldsymbol{f}$ is symmetric tensor function.

Newtonian fluids have the property that there is a linear dependence between $\boldsymbol{t}$ and $\mathbf{D}$. The constitutive equation for incompressible viscous fluids is

$$\boldsymbol{t} = -p(\boldsymbol{x}, t)\mathbf{I} + 2\mu\mathbf{D}, \tag{2.16}$$

and $\boldsymbol{I}$ is identity tensor, μ is shear viscosity (resistance of fluid to shear).

Stress vector for viscous fluids is given by [1]

$$\boldsymbol{t} = -p\boldsymbol{n} + \mu\big[2(\boldsymbol{n} \cdot \nabla)\mathbf{v} + \boldsymbol{n} \times (\nabla \times \mathbf{v})\big]. \tag{2.17}$$

Navier-Stokes equations

Navier-Stokes equations describe the motion of an incompressible Newtonian fluid. Their form is given in the following Lemma.

Lemma 2.1.4. *Motion of an incompressible Newtonian fluid is described by the following system of equations:*

$$\nabla \cdot \mathbf{v} = 0, \tag{2.18}$$

$$\frac{\partial \mathbf{v}}{\partial t} + (\mathbf{v} \cdot \nabla)\mathbf{v} = -\frac{1}{\rho}\nabla p + \nu \nabla^2 \mathbf{v} + \mathbf{g}, \tag{2.19}$$

where constants ρ and μ represent density and shear viscosity respectively, $\mathbf{g}$ *is gravitational acceleration and $\nu = \mu/\rho$ is kinematic viscosity.*

Proof. Since the fluid is incompressible, equation (2.18) is a direct consequence of this property following from the mass balance law. Equation (2.19) is the momentum balance law (2.14) applied to Incompressible Newtonian fliuds in the following way:

1. body forces are due to gravity only, $\boldsymbol{b} = \mathbf{g}$;
2. divergence of the stress tensor reads

$$\operatorname{div} \boldsymbol{T} = \operatorname{div}(-p\boldsymbol{I} + 2\mu\mathbf{D}) = -\nabla p + \mu\left(\nabla^2 \mathbf{v} + \nabla(\nabla \cdot \mathbf{v})\right).$$

Note that the last term vanishes due to equation (2.18), and equation (2.19) follows. □

2.2 Derivation of the Washburn's equation

The equation for capillary rise phenomenon in a tube was first proposed by Green and Ampt [11] and later independently developed by Lucas [19] and Washburn [32]. The Washburn's (Lucas-Washburn) equation may also be referred to as capillary model in the porous media literature, since a porous medium is modelled as a bundle of aligned capillary tubes [21]. The terms that occur in the governing equation are inertial, gravitational, viscous and capillary.

The main approach that was used to derive and modify Washburn's was applying momentum balance to control volume inside the capillary tube. [16],[4], [22]

The transition in flow pattern between different zones are also studied [9], [24], [28]. Such studies show that inertial forces are dominant at the very beginning of capillarity. The gravity effects are significant near the equilibrium height (i.e. when liquid column stops rising) [8].

In this thesis, we derive Wasburn's equation with using balance laws. We use assumptions about Poisseuille flow for Newtonian incompressible fluid, neglecting the friction.

In this thesis Washburn's equation will be derived from the first principle. This means that we shall use mass and mometum balance equations for the motion of an incompressible Newtonian fluid through the vertical pipe of constant circular cross section. Our derivation will have two steps. Firstly, we shall analyze the motion by means of local balance laws under physically motivated assumptions. This will lead to a simplification in the structure of unknown fields of velocity $\mathbf{v}$ and pressure p. Secondly, using the results of local analysis we shall formulate the momentum balance law in global form and derive the Washburn's equation.

2.2.1 Balance Equations in polar cylindrical coordinates

In our model of capillary rise in a pipe, we analyse the model in polar-cylindrical coordinates r, φ, z:

$$\begin{aligned} 0 \leq & r \leq R, \\ 0 \leq & \varphi \leq 2\pi, \\ 0 \leq & z \end{aligned}$$

We introduce a positively oriented orthonormal basis

$$\{\mathbf{e}_r, \mathbf{e}_\varphi, \mathbf{e}_z\}.$$

It can be shown that mass balance equation in polar cylindrical coordinates is given as [15]

$$\frac{1}{r}\frac{\partial}{\partial r}(r v_r) + \frac{1}{r}\frac{\partial v_\varphi}{\partial \varphi} + \frac{\partial v_z}{\partial z} = 0. \tag{2.20}$$

Moreover, momentum balance equations in polar cylindrical coordinates can be written as [15].

$$\begin{aligned} \frac{\partial v_r}{\partial t} + (\mathbf{v}\cdot\nabla)v_r - \frac{v_\varphi^2}{r} &= -\frac{1}{\rho}\frac{\partial p}{\partial r} + \nu\left(\nabla^2 v_r - \frac{v_r}{r^2} - \frac{2}{r^2}\frac{\partial v_\varphi}{\partial \varphi}\right), \\ \frac{\partial v_\varphi}{\partial t} + (\mathbf{v}\cdot\nabla)v_\varphi + \frac{v_r v_\varphi}{r} &= -\frac{1}{\rho r}\frac{\partial p}{\partial \varphi} + \nu\left(\nabla^2 v_\varphi - \frac{v_\varphi}{r^2} + \frac{2}{r^2}\frac{\partial v_r}{\partial \varphi}\right), \\ \frac{\partial v_z}{\partial t} + (\mathbf{v}\cdot\nabla)v_z &= -\frac{1}{\rho}\frac{\partial p}{\partial z} + \nu\nabla^2 v_z - g. \end{aligned} \tag{2.21}$$

The following relations in cylindrical coordinates will be of interest in our derivation:

$$\begin{aligned} \nabla &= \frac{\partial}{\partial r}\mathbf{e}_r + \frac{1}{r}\frac{\partial}{\partial \varphi}\mathbf{e}_\varphi + \frac{\partial}{\partial z}\mathbf{e}_z, \\ \mathbf{v}\cdot\nabla &= v_r\frac{\partial}{\partial r} + \frac{v_\varphi}{r}\frac{\partial}{\partial \varphi} + v_z\frac{\partial}{\partial z}, \\ \nabla^2 &= \frac{1}{r}\frac{\partial}{\partial r}\left(r\frac{\partial}{\partial r}\right) + \frac{1}{r^2}\frac{\partial^2}{\partial \varphi^2} + \frac{\partial^2}{\partial z^2}. \end{aligned}$$

2.2.2 Local Analysis – Assumptions

Local analysis of balance laws will be concenrned with basic assumptions about flow fields, and appropriate consequences and simplifications.

1. **Velocity field** in orthonormal basis is expressed as

$$\mathbf{v} = v_r\mathbf{e}_r + v_\varphi\mathbf{e}_\varphi + v_z\mathbf{e}_z.$$

It will be assumed that the fluid flows along the z-axis only, and therefore

$$v_r \equiv 0, \quad v_\varphi \equiv 0. \tag{2.22}$$

Moreover, we will assume the axial symmetry of flow around an z-axis. Thus, velocity field of the fluid does not depend on φ. Therefore, the z-component of the velocity depends on r and z (and time t) only

$$v_z = v_z(r, z, t) \tag{2.23}$$

Consequences of the assumptions about the velocity field are:

(a) Due to assumption (2.22), mass balance equation (2.20) reduces to $\partial v_z/\partial z = 0$. Thus, velocity field is independent of z, $v_z = v_z(r, t)$.

(b) Due to the same assumption (2.22), momentum balance equations $(2.21)_{1-2}$ are reduced to: $\partial p/\partial r = 0$ and $\partial p/\partial \varphi = 0$. Consequently, the pressure field is $p = p(z, t)$.

2. Next, we assume that the motion of the fluid is described by the **Poisseuille flow**, which means parabolic profile of the local velocity field

$$v_z(r, t) = v(t)\left(1 - \frac{r^2}{R^2}\right). \tag{2.24}$$

This is standard assumption for the motion of Newtonian fluid in this case [34]. It is valid for the developed flow of the fluid throughout the volume, except in the small neighbourhood of free surface. Since our free surface is small compared to the area of contact of water column with the side of a cylinder, influence of the velocity field in its neighbourhood will be negligible on the overall motion.

3. **Pressure field** is assumed to be stationary, i.e. it depends only on z-coordinate

$$p = p(z). \tag{2.25}$$

2.2.3 Global Analysis – Derivation

In order to apply global form of balance equations, we will present the pipe in polar cylindrical coordinates. The volume occupied by the fluid will be described as the the set $V(t)$ in polar cylindrical coordinates

$$V(t) = \{(r, \varphi, z) | r \in [0, R], \varphi \in [0, 2\pi], z \in [0, h(t)]\},$$

where $h(t)$ is the height reached by the fluid column.

We will split the boundary of our region of interest in three parts, namely,

$$\partial V = \partial V_1(t) \cup \partial V_2 \cup \partial V_3;$$

so that ∂V_1 and ∂V_3 are the boundaries of bottom and top bases of the cylinder, respectively, ∂V_2 is the boundary of the cylinder's side:

$$\begin{aligned}
\partial V_1 &= \{(r, \varphi, z) | r \in [0, R], \varphi \in [0, 2\pi], z = 0\}, && \boldsymbol{n_1} = -\boldsymbol{e_z};\\
\partial V_2 &= \{(r, \varphi, z) | r = R, \varphi \in [0, 2\pi], z \in [0, h(t)]\}, && \boldsymbol{n_2} = \boldsymbol{e_r};\\
\partial V_3 &= \{(r, \varphi, z) | r \in [0, R], \varphi \in [0, 2\pi], z = h(t)\}, && \boldsymbol{n_3} = \boldsymbol{e_z}.
\end{aligned}$$

Unit normal vectors $\boldsymbol{n_1}$, $\boldsymbol{n_2}$ and $\boldsymbol{n_3}$ are given with respect to the orthonormal basis (see Figure 2.3).

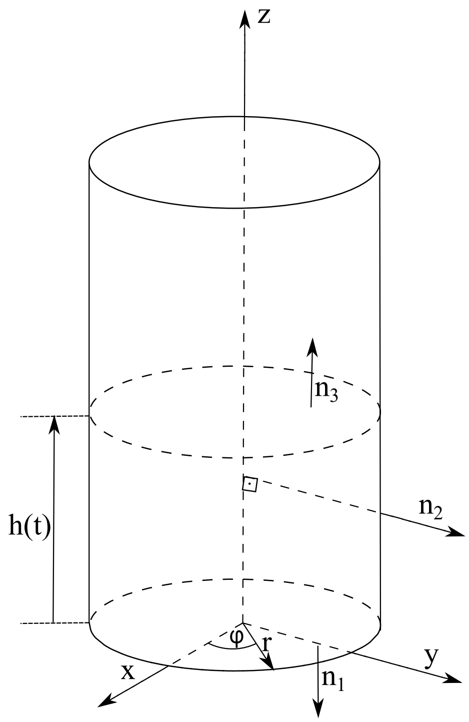

Figure 2.3. Representation of the pipe in the cylindrical coordinates

Due to our assumption, body force depends only on gravity

$$\boldsymbol{b} = \mathbf{g} = -g\boldsymbol{e_z}.$$

Our goal is to apply the momentum balance in global form (2.12)

$$\frac{d}{dt}\int_{P_t} \boldsymbol{K}(\boldsymbol{x},t)dV = \int_{\partial\mathcal{P}_t} \boldsymbol{t(n)}dA + \int_{\mathcal{P}_t} \rho\boldsymbol{b}dV,$$

to the volume $V(t)$, taking into accout assumptions and their consequences from the previous Section. We will calculate separately the right and the left hand side of the equation. Firstly, the mean velocity needed for further calculations will be introduced.

Mean velocity

We take the average value of the velocity field $\mathbf{v}$ with respect to cylindric cross section and apply the assumption about Poisseuille flow

$$\bar{v}(t) = \frac{1}{R^2\pi}\int_0^{2\pi}\int_0^R v_z(t,r)rdrd\varphi = \frac{1}{R^2\pi}\int_0^{2\pi}\int_0^R v(t)\left(1-\frac{r^2}{R^2}\right)rdrd\varphi. \qquad (2.26)$$

Fubini's theorem implies that

$$\frac{1}{R^2\pi}\int_0^{2\pi}\int_0^R v(t)\left(1-\frac{r^2}{R^2}\right) r dr d\varphi = \frac{v(t)}{R^2\pi}\int_0^R \left(r-\frac{r^3}{R^2}\right) dr \int_0^{2\pi} d\varphi = 2\pi\frac{v(t)}{R^2\pi}\frac{R^2}{4}$$

Finally,

$$\bar{v}(t) = \frac{1}{2}v(t). \tag{2.27}$$

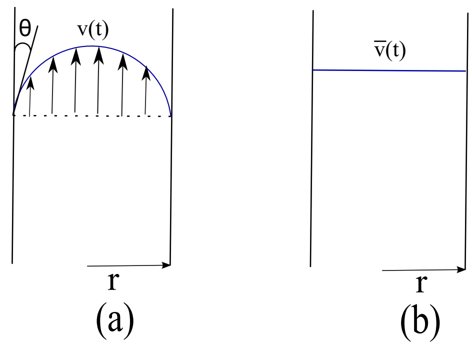

Figure 2.4. Poisseuille flow with concave meniscus (a) and mean velocity approximation with flat meniscus (b).

Left hand side

The momentum is given by

$$\boldsymbol{K}(\boldsymbol{x},t) = \rho(\boldsymbol{x},t)\mathbf{v}(\boldsymbol{x},t) = \rho v_z(r,t)\mathbf{e}_z,$$

since in our case velocity field has only z-component, that depends on r and t. Thus, the left hand side of (2.12) is

$$\frac{d}{dt}\int_{V(t)} \boldsymbol{K}(\boldsymbol{x},t)dV = \frac{d}{dt}\int_{V(t)} \rho v_z(r,z)\mathbf{e}_z dV = \rho\left[\frac{d}{dt}\int_0^{h(t)}\int_0^R\int_0^{2\pi} v_z(r,t)d\varphi r dr dz\right]\mathbf{e}_z.$$

In order to simplify further calculation, we introduce **mean velocity**. The physical interpretation is that the shape of meniscus is not parabolic, but flat. Moreover, this will enable to establish the relation with usual/simplified derivation of Washburn's equation present in the literature. From (2.26), by applying Fubini's theorem we have

$$\int_0^R\int_0^{2\pi} v_z(r,t)d\varphi r dr = R^2\pi\bar{v}(t),$$

and it follows that

$$\begin{aligned}\frac{d}{dt}\int_{V(t)} \boldsymbol{K}(\boldsymbol{x},t)dV &= \rho R^2\pi\left[\frac{d}{dt}\int_0^{h(t)}\bar{v}(t)dz\right]\mathbf{e}_z = \rho R^2\pi\left[\int_0^{h(t)}\dot{\bar{v}}(t)dz + \bar{v}(t)\dot{h}(t) + 0\right]\mathbf{e}_z \\ &= \rho R^2\pi\left[\dot{\bar{v}}(t)h(t) + \bar{v}(t)\dot{h}(t)\right]\mathbf{e}_z = \rho R^2\pi\frac{d}{dt}\left[\bar{v}(t)h(t)\right]\mathbf{e}_z.\end{aligned} \tag{2.28}$$

Right hand side

In order to calculate force per unit volume $\boldsymbol{F}_v$, we integrate body force over volume

$$\boldsymbol{F}_v = \int_{V(t)} \rho \boldsymbol{b} dV = \int_{V(t)} \rho(-g\boldsymbol{e_z})dV = -\rho g \boldsymbol{e_z} \int_{V(t)} dV = -\rho g \boldsymbol{e_z} \int_0^{h(t)} \int_0^R \int_0^{2\pi} r dr d\varphi dz.$$

Evaluating integrals with Fubini's theorem

$$\int_0^{h(t)} dz \int_0^R r dr \int_0^{2\pi} d\varphi = h(t)\frac{R^2}{2}2\pi = R^2\pi h(t),$$

gives us that

$$\boldsymbol{F}_v = \int_{V(t)} \rho \boldsymbol{b} dV = -\rho g R^2 \pi h(t) \boldsymbol{e_z}. \tag{2.29}$$

It is left to determine the total contact force $\boldsymbol{F}_s$ by integrating traction over the boundary of our pipe. Since we have divided the boundary into three regions, it follows from (2.11) that

$$\boldsymbol{F}_s = \int_{\partial V} \boldsymbol{t} dS = \int_{\partial V_1} \boldsymbol{t_1} dS_1 + \int_{\partial V_2} \boldsymbol{t_2} dS_2 + \int_{\partial V_3} \boldsymbol{t_3} dS_3$$

where S_1, S_2 and S_3 are surface elements, given by

$$\begin{aligned} dS_1 &= r dr d\varphi, \\ dS_2 &= R d\varphi dz, \\ dS_3 &= r dr d\varphi. \end{aligned}$$

We further use (2.17).

$$\nabla = \frac{\partial}{\partial r}\mathbf{e}_r + \frac{1}{r}\frac{\partial}{\partial \varphi}\mathbf{e}_\varphi + \frac{\partial}{\partial z}\mathbf{e}_z$$

In our case $\mathbf{v} = v_z \mathbf{e}_z$. Therefore,

$$\nabla \times \mathbf{v} = \operatorname{curl} \mathbf{v} = \frac{1}{r}\begin{vmatrix} \mathbf{e}_r & r\mathbf{e}_r & \mathbf{e}_z \\ \frac{\partial}{\partial r} & \frac{\partial}{\partial \varphi} & \frac{\partial}{\partial z} \\ v_r & r v_\varphi & v_z \end{vmatrix} = \begin{vmatrix} \mathbf{e}_r & r\mathbf{e}_r & \mathbf{e}_z \\ \frac{\partial}{\partial r} & \frac{1}{r}\frac{\partial}{\partial \varphi} & \frac{\partial}{\partial z} \\ 0 & 0 & v_z \end{vmatrix} = \frac{1}{r}\frac{\partial v_z}{\partial \varphi}\mathbf{e}_r - \frac{\partial v_z}{\partial r}\mathbf{e}_\varphi = -\frac{\partial v_z}{\partial r}\mathbf{e}_\varphi$$

Our goal is to determine components of the stress tensor, $\boldsymbol{t_1}$, $\boldsymbol{t_2}$ and $\boldsymbol{t_3}$.

$$\boldsymbol{t_1} = -p\boldsymbol{n_1} + \mu\big[2(\boldsymbol{n_1}\cdot\nabla)\mathbf{v} + \boldsymbol{n_1}\times(\nabla\times\mathbf{v})\big]$$

$$(\boldsymbol{n_1}\cdot\nabla)\mathbf{v} = (-\mathbf{e}_z\cdot\nabla)(v_z\mathbf{e}_z) = -\frac{\partial v_z}{\partial z}\mathbf{e}_z = 0$$

$$\boldsymbol{n_1}\times(\nabla\times\mathbf{v}) = (-\mathbf{e}_z)\times(-\frac{\partial v_z}{\partial r})\mathbf{e}_\varphi$$

Therefore,

$$\boldsymbol{t_1} = p\mathbf{e}_z - \mu\frac{\partial v_z}{\partial r}\mathbf{e}_r$$

Similarly,

$$\boldsymbol{t_2} = -p\boldsymbol{n_r} + \mu\big[2(\boldsymbol{n_2}\cdot\nabla)\mathbf{v} + \boldsymbol{n_2}\times(\nabla\times\mathbf{v})\big].$$

$$(\boldsymbol{n_2}\cdot\nabla)\mathbf{v} = (\mathbf{e}_r\cdot\nabla)(v_z\mathbf{e}_z) = \frac{\partial v_z}{\partial r}\mathbf{e}_z$$

$$\boldsymbol{n_2}\times(\nabla\times\mathbf{v}) = \mathbf{e}_r\times\left(-\frac{\partial v_z}{\partial r}\mathbf{e}_\varphi\right) = -\frac{\partial v_z}{\partial r}\left(\mathbf{e}_r\times\mathbf{e}_\varphi\right) = -\frac{\partial v_z}{\partial r}\mathbf{e}_z,$$

therefore,

$$\boldsymbol{t_2} = -p\mathbf{e}_r + \mu\left[2\frac{\partial v_z}{\partial r}\mathbf{e}_z - \frac{\partial v_z}{\partial r}\mathbf{e}_z\right] = -p\mathbf{e}_r + \mu\frac{\partial v_z}{\partial r}\mathbf{e}_z$$

Note that $\boldsymbol{t_3}$ equals $-\boldsymbol{t_1}$

$$\boldsymbol{t_3} = -p\mathbf{e}_z + \mu\frac{\partial v_z}{\partial r}\mathbf{e}_r$$

Taking into account computations given above, we compute the net force exerted on the cylinder bases:

$$\int_{\partial V_1}\boldsymbol{t_1}dS_1 = \int_0^R\int_0^{2\pi}\boldsymbol{t_1}rdrd\varphi = R^2\pi p(0)\mathbf{e_z} - 2\pi\mu\left[\int_0^R r\frac{\partial v_z}{\partial r}dr\right]\mathbf{e_z},$$

$$\int_{\partial V_3}\boldsymbol{t_3}dS_3 = -R^2\pi p(h(t))\mathbf{e_z} + 2\pi\mu\left[\int_0^R r\frac{\partial v_z}{\partial r}\right]dr\mathbf{e_z},$$

and thus

$$\int_{\partial V_1}\boldsymbol{t_1}dS_1 + \int_{\partial V_3}\boldsymbol{t_3}dS_3 = \mathbf{0} + R^2\pi\Big[p(0) - p(h(t))\Big]\mathbf{e}_z.$$

We now consider the net force exerted upon the cylinder's side

$$\int_{\partial V_2}\boldsymbol{t_2}dS_2 = -\left[\int_0^{2\pi}\int_0^{h(t)}p(z)\mathbf{e_r}Rd\varphi dz\right] + 2\mu\pi R\left[\int_0^{h(t)}\left(\frac{\partial v_z}{\partial r}\right)dz\right]\mathbf{e_z}.$$

Note that unit vector $\mathbf{e_r}$ must be kept under the integral sign because it is not constant. To compute the first integral, we use $\mathbf{e_r} = \cos(\varphi)\,\mathbf{e_x} + \sin(\varphi)\,\mathbf{e_y}$ and apply Fubini's theorem

$$\begin{aligned}\int_0^{2\pi}\int_0^{h(t)}p(z)\mathbf{e_r}Rd\varphi dz &= \int_0^{2\pi}\int_0^{h(t)}p(z)\left(\cos(\varphi)\,\mathbf{e_x} + \sin(\varphi)\,\mathbf{e_y}\right)Rd\varphi dz\\ &= \left[\int_0^{2\pi}\int_0^{h(t)}p(z)\cos(\varphi)\,Rd\varphi dz\right]\mathbf{e_x} + \left[\int_0^{2\pi}\int_0^{h(t)}p(z)\sin(\varphi)\,Rd\varphi dz\right]\mathbf{e_y}\\ &= R\left[\int_0^{h(t)}p(z)\left(\int_0^{2\pi}\cos(\varphi)\,d\varphi\right)dz\right]\mathbf{e_x} + R\left[\int_0^{h(t)}p(z)\left(\int_0^{2\pi}\sin(\varphi)\,d\varphi\right)dz\right]\mathbf{e_y}\\ &= \mathbf{0}.\end{aligned}$$

In order to evaluate the second term, we will use the assumption about Poisseuille flow

$$\begin{aligned}
2\mu\pi R\left[\int_0^{h(t)}\left(\frac{\partial v_z}{\partial r}\right)dz\right]\mathbf{e}_z &= 2\mu\pi R\left[\int_0^{h(t)}\frac{\partial}{\partial r}\left(v(t)-\frac{v(t)r^2}{R^2}\right)dz\right]\mathbf{e_z}\\
&= -2\mu\pi R\int_0^{h(t)}\left[\frac{2rv(t)}{R^2}\right]\mathbf{e_z} = -2\mu\pi R\int_0^{h(t)}\left[\frac{4r\bar{v}(t)}{R^2}dz\right]\mathbf{e_z}\\
&= -\frac{8\mu\pi r\bar{v}(t)h(t)}{R}\mathbf{e_z} = -8\mu\pi\bar{v}(t)h(t)\mathbf{e_z}.
\end{aligned}$$

The last equality follows when $r = R$ is plugged in. Finally,

$$\int_{\partial V_2}\boldsymbol{t_2}dS_2 = -8\mu\pi\bar{v}(t)h(t)\mathbf{e}_z.$$

Thus, the total contact force is

$$\boldsymbol{F}_s = \int_{V(t)}\boldsymbol{t}dS = -R^2\pi\Big[p(h(t)) - p(0)\Big]\mathbf{e}_z - 8\mu\pi\bar{v}(t)h(t)\mathbf{e}_z \tag{2.30}$$

Washburn's equation

Firstly, we substitute left and right hand side into the global form of momentum balance equation

$$\frac{d}{dt}\int_{V(t)}\boldsymbol{K}(\boldsymbol{x},t)dV = \boldsymbol{F}_v + \boldsymbol{F}_s;$$

that is

$$\rho R^2\pi\frac{d}{dt}\Big[\bar{v}(t)h(t)\Big]\mathbf{e}_z = -\rho g R^2\pi h(t)\boldsymbol{e_z} - R^2\pi\Big[p(h(t)) - p(0)\Big]\mathbf{e}_z - 8\mu\pi\bar{v}(t)h(t)\mathbf{e}_z.$$

Divide both sides by $-R^2\pi\mathbf{e}_z$ and substitute $\bar{v}(t) = \frac{dh}{dt} = \dot{h}(t)$, (since rate of change of height in the pipe equals velocity),

$$-\rho\frac{d}{dt}\Big[\dot{h}(t)h(t)\Big] = \rho g h(t) + \Big[p(h(t)) - p(0)\Big] + \frac{8\mu\dot{h}(t)h(t)}{R^2},$$

equivalently,

$$\Big[p(0) - p(h(t))\Big] = \rho\frac{d}{dt}\Big[\dot{h}(t)h(t)\Big] + \rho g h(t) + \frac{8\mu\dot{h}(t)h(t)}{R^2}, \tag{2.31}$$

The last thing we introduce is the surface tension. The general formula is

$$\gamma = \frac{F}{d}$$

where F is force intensity due to surface tension, d is length along which the force is felt and γ is the coefficient of surface tension. In our case, force due to surface tension acts along the inner circumference of the pipe, it follows that

$$F = 2R\pi\gamma.$$

Since we are considering water flow with respect to z-coordinate, we will need only the vertical component of the surface tension force

$$F_{vert} = F\cos\theta = 2R\pi\gamma\cos\theta,$$

where θ is the contact angle of fluid with meniscus. On the other hand, pressure has only z-component and difference in pressure balances with vertical component of surface tension

$$p(0) - p(h(t)) = \frac{F_{vert}}{R^2\pi} = \frac{2\gamma\cos\theta}{R}.$$

We plug the last expression in (2.31) and finally obtain Washburn's equation

$$\rho\frac{d}{dt}\left[\dot{h}(t)h(t)\right] + \rho g h(t) + \frac{8\mu\dot{h}(t)h(t)}{R^2} = \frac{2\gamma\cos\theta}{R}. \tag{2.32}$$

2.3 Scaling of the Washburn's equation

Consider the governing equation

$$\frac{8\mu}{R^2}(h+h_0)h' + \rho g h + \left[\rho(h+h_0)h'\right]' = \frac{2\gamma\cos(\theta)}{R} \tag{2.33}$$

with initial conditions

$$h(0) = \alpha h_e, \quad h'(0) = 0, \tag{2.34}$$

where prime ($'$) denotes differentiation with respect to time, $h(t)$ is column height at time t, h_0 is the immersion height of the tube below the free surface of liquid outside the tube (see Figure 2.5), h_e is the equilibrium height, and parameter α depends on the experimental set-up ($0 < \alpha < 1$).

Equilibrium height h_e is determined as particular solution of equation (2.33), $h(t) = h_e = \text{const.}$

$$\rho g h_e = \frac{2\gamma\cos(\theta)}{R},$$

and expresses the balance between hydrostatic and capillary forces. It reads

$$h_e = \frac{2\gamma\cos(\theta)}{\rho g R}. \tag{2.35}$$

Equilibrium height is also known as Jurin's height.

In order to simplify further analysis i.e. reduce number of parameters, we will transform the equation (2.33) into dimensionless form as in [23]. We introduce $\tilde{h}$ as:

$$\tilde{h}(t) = h(t) + h_0. \tag{2.36}$$

It follows that (2.33) transforms as

$$\frac{8\mu}{R^2}\tilde{h}\tilde{h}' + \rho g(\tilde{h} - h_0) + \left[\rho\tilde{h}h'\right]' = \frac{2\gamma\cos(\theta)}{R}$$

that is,

$$\frac{8\mu}{R^2}\tilde{h}\tilde{h}' + \rho g\tilde{h} + \left[\rho\tilde{h}h'\right]' = \frac{2\gamma\cos(\theta)}{R} + \rho g h_0 \tag{2.37}$$

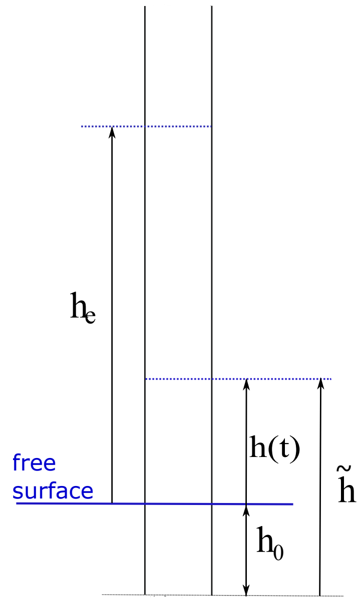

Figure 2.5. The pipe with free surface of liquid (red line), immersion height h_0, equilibrium height h_e, $h(t)$ column level at time t and $\tilde{h} = h(t) + h_0$.

For casting height and time, we use the following scale

$$H = \frac{\tilde{h}}{h_e}, \quad T = \frac{t}{\tau}. \tag{2.38}$$

Note that the scale for time - constant τ will be determined later.
Next, we plug (2.38) into (2.33):

$$\frac{8\mu}{R^2} \cdot h_e H \cdot \frac{d}{\tau dT}(h_e H) + \rho g \cdot h_e H + \rho \cdot \frac{d}{\tau dT}\left(h_e H \cdot \frac{d}{\tau dt}(h_e H)\right) = \frac{2\gamma \cos(\theta)}{R} + \rho g h_0,$$

that is,

$$\frac{8\mu h_e^2}{\tau R^2} H H' + \rho g h_e H + \frac{\rho h_e^2}{\tau^2} (H H')' = h_e \rho g + \rho g h_0.$$

Divide both sides by $h_e \rho g$ in order to get:

$$\frac{8\mu h_e}{R^2 \rho g \tau} H H' + H + \frac{h_e}{g\tau^2} (H H')' = 1 + D,$$

where

$$D = \frac{h_0}{h_e}. \tag{2.39}$$

Since the main balance usually occures between the capillary and hydrostatic forces, we choose

$$\frac{8\mu h_e}{R^2 \rho g \tau} = 1,$$

that is

$$\tau = \frac{8\mu h_e}{R^2 \rho g}. \tag{2.40}$$

Finally, our scaled equation is:

$$HH' + H + \omega(HH')' = 1 + D, \tag{2.41}$$

with initial conditions

$$H(0) = \alpha, \quad H'(0) = 0. \tag{2.42}$$

where dimensionless parameter ω we introduce as:

$$\omega = \frac{h_e}{g\tau^2} = \frac{\rho^2 R^4 g}{64\mu^2 h_e}. \tag{2.43}$$

Remark about initial conditions. The initial conditions (2.34), or (2.42) in dimensionless form, are chosen such that fluid initially penetrated the column, $\alpha > 0$, but the velocity is zero at the beginning of the flow. This choice differs from the ones that prevail in the literature. Namely, it is common to adopt initial height to be zero [23], $\alpha = 0$. This choice creates a singularity in the Washburn's equation (2.41) at $t = 0$, since H'' is multiplied by H. To avoid the singularity, $H'(0)$ is determined from the differential equation.

Our opinion is that this choice of initial conditions contradicts the basic principles upon which the model is derived, i.e. that the state of the system (position and velocity) and actions upon it determine its subsequent evoution. In other words, initial conditions have to be imposed independently of the governing equation. This standpoint motivated us to choose alternative form of initial conditions (2.42) that remove the singularity. However, to mimic the real situation as much as possible, which means that initial height of the fluid is negligibly small, we shall assume $0 < \alpha \ll 1$.

To remove the singularity caused by zero initial height at $t = 0$, it is needed to analyze more thoroughly the initial phase of the motion, and possibly change the model.

Chapter 3

Existence and Uniqueness

In this Chapter we firstly transform scaled Washburn's equation into ordinary differential equation of second order, where nonlinearity involves only the function and not its derivatives. Next, we use general initial conditions to show that solution of transformed equation (if exists) satisfies the integral equation proposed in [23]. Energy estimate gave us bounds on a solution, that appears to be always positive. That is sufficient condition to apply Banach fixed point theorem, in order to formally prove existence and uniqueness of the solution of transformed equation. Finally, we determine domain and range of a solution, depending on initial height of a liquid column and immersion depth.

3.1 Transformation of the Washburn's equation

We start this section by statement and proof of Lemma 1 from [23], the only difference is in initial conditions.

Lemma 3.1.1. *The problem*

$$HH' + H + \omega(HH')' = 1 + D \tag{3.1}$$

with

$$H(0) = \alpha, \quad H'(0) \tag{3.2}$$

can be transformed via $u(s) = \frac{1}{2}H(T)^2$ *with* $s = \frac{T}{\sqrt{\omega}}$ *into*

$$u'' + \frac{1}{\sqrt{\omega}}u' + \sqrt{2u} = 1 + D, \tag{3.3}$$

with

$$u(0) = \frac{1}{2}\alpha^2, \quad u'(0) = 0, \tag{3.4}$$

for $0 < \alpha << 1$ *and independent variable* s.

Proof. If we choose $u(s) = \frac{1}{2}H(T)^2 = \frac{1}{2}H(s\sqrt{\omega})^2$, it follows that

$$u'(s) = \sqrt{\omega}H(s\sqrt{\omega})H'(s\sqrt{\omega}).$$

$$\frac{d}{dT} = \frac{d}{ds}\frac{ds}{dT} = \frac{1}{\sqrt{\omega}}\frac{d}{ds}$$

Plug expressions for $u(s)$ and $u'(s)$ into (3.1)

$$\frac{1}{\sqrt{\omega}}u'(s) + \sqrt{2u} + \omega\left(\frac{1}{\sqrt{\omega}}u'(s)\right)' = 1 + D,$$

since

$$\omega\frac{d}{dT}\left(\frac{1}{\sqrt{\omega}}\frac{du'(s)}{ds}\right) = \sqrt{\omega}\frac{d}{dT}\left(\frac{du'(s)}{ds}\right) = \sqrt{\omega}\frac{1}{\sqrt{\omega}}\frac{du'(s)}{ds} = u''(s),$$

it follows that

$$u''(s) + \frac{1}{\sqrt{\omega}}u'(s) + \sqrt{2u} = 1 + D.$$

Let us transform initial conditions (2.34). Consider

$$H(0) = a = \alpha \in (0,1), \quad H'(0) = 0.$$

We transform initial conditions such that

$$u(0) = \frac{1}{2}H(0)^2 = \frac{1}{2}\alpha^2, \quad u'(0) = \sqrt{\omega}H(0)H'(0) = 0. \tag{3.5}$$

where $0 < \alpha << 1$. This is because the expected maximum value of our scaled height $\sup H(T) = O(1)$, and initial height should be small positive parameter. □

This transformation is useful since nonlinearity involves only the function u but not its derivatives. The next Lemma will be helpful for rewriting the equation (3.3) into integral form.

Lemma 3.1.2. *Every equation of the form*

$$y'' + \beta y' + f(y) = 0 \tag{3.6}$$

can be written as

$$z'' + \Phi(x,z) = 0. \tag{3.7}$$

Proof. Multiply both sides of (3.6) by $e^{\beta x}$:

$$e^{\beta x}y'' + \beta e^{\beta x}y' + e^{\beta x}y = 0,$$

equivalently,

$$\frac{d}{dx}\left(e^{\beta x}y'\right) + e^{\beta x}y = 0.$$

Let $z(x) = e^{\beta x}y(x)$. It follows that

$$y(x) = e^{-\beta x}z(x),$$

that is,

$$f(y) = f(e^{-\beta x}z).$$

Thus,

$$e^{\beta x}f(y) = e^{\beta x}f(e^{-\beta x}z) =: \Phi(x,z).$$

The claim (3.7) follows. □

The Theorem 1 from [23] will be divided into three parts, and proven step by step in this section.

Integral form of Washburn's equation

Theorem 3.1.3. *Let $u = u(s)$ be a solution of equation (3.3) with initial conditions (3.5). The function u is a solution of an integral equation*

$$u(s) = \frac{1}{2}\alpha^2 + \int_0^s \left(1 + D - \sqrt{2u(t)}\right) G(s-t)dt, \tag{3.8}$$

where

$$G(z) = \sqrt{\omega}\left(1 - e^{-\frac{z}{\sqrt{\omega}}}\right). \tag{3.9}$$

Proof. Using the similar idea (as in the proof of Lemma 3.1.2), we multiply both sides of (3.3) by $e^{\frac{s}{\sqrt{\omega}}}$:

$$e^{\frac{s}{\sqrt{\omega}}}u'' + \frac{1}{\sqrt{\omega}}e^{\frac{s}{\sqrt{\omega}}}u' + e^{\frac{s}{\sqrt{\omega}}}\sqrt{2u} = e^{\frac{s}{\sqrt{\omega}}}.$$

Equivalently,

$$\frac{d}{ds}\left(e^{\frac{s}{\sqrt{\omega}}}u'\right) = e^{\frac{s}{\sqrt{\omega}}}\left(1 - \sqrt{2u}\right). \tag{3.10}$$

Let $f(u) = 1 + D - \sqrt{2u}$. Integrate both sides of (3.10) from 0 to s

$$\int_0^s d(e^{\frac{t}{\sqrt{\omega}}}u') = \int_0^s e^{\frac{t}{\sqrt{\omega}}}f(u(t))dt. \tag{3.11}$$

Next, evaluate integral on the left hand side, using Newton-Leibniz formula,

$$\int_0^s d(e^{\frac{t}{\sqrt{\omega}}}u') = e^{\frac{t}{\sqrt{\omega}}}u'(t)\Big|_0^s = e^{\frac{s}{\sqrt{\omega}}}u'(s) - u'(0) = e^{\frac{s}{\sqrt{\omega}}}u'(s),$$

since from (3.5), $u'(0) = 0$. Thus, (3.11) becomes

$$e^{\frac{s}{\sqrt{\omega}}}u'(s) = \int_0^s e^{\frac{t}{\sqrt{\omega}}}f(u(t))dt,$$

that is,

$$u'(s) = e^{-\frac{s}{\sqrt{\omega}}}\int_0^s e^{\frac{t}{\sqrt{\omega}}}f(u(t))dt. \tag{3.12}$$

Since s is independent variable, we introduce the change of variables $s \to z$.

$$u'(z) = \frac{du(z)}{dz} = e^{-\frac{z}{\sqrt{\omega}}}\int_0^z e^{\frac{t}{\sqrt{\omega}}}f(u(t))dt = \psi(z),$$

simplified,

$$du(z) = \psi(z)dz. \tag{3.13}$$

Integrate (3.13) from 0 to s

$$\int_0^s du(z) = \int_0^s \psi(z)dz;$$

left hand side equals to

$$\int_0^s du(z) = u(z)\Big|_0^s = u(s) - u(0) = u(s) - \frac{1}{2}\alpha^2, \tag{3.14}$$

therefore,

$$u(s) - \frac{1}{2}\alpha^2 = \int_0^s \psi(z)dz = \int_0^s e^{-\frac{z}{\sqrt{\omega}}} \left(\int_0^z e^{\frac{t}{\sqrt{\omega}}} f(u(t))dt \right) dz \tag{3.15}$$

The next step is to rewrite the right hand side as a Green's function. Let

$$\int_0^z e^{\frac{t}{\sqrt{\omega}}} f(u(t))dt = F(z) - F(0), \tag{3.16}$$

where $F(z)$ is a primitive function. The right hand side becomes

$$\int_0^s e^{-\frac{z}{\sqrt{\omega}}} \left(\int_0^z e^{\frac{t}{\sqrt{\omega}}} f(u(t))dt \right) dz = \int_0^s e^{-\frac{z}{\sqrt{\omega}}} \left(F(z) - F(0)\right) dz;$$

use partial integration with

$$u = F(z) - F(0), \quad du = F'(z)dz,$$
$$v = -\sqrt{\omega}e^{-\frac{z}{\omega}}, \quad dv = e^{-\frac{z}{\sqrt{\omega}}} dz,$$

thus

$$\begin{aligned} \int_0^s e^{-\frac{z}{\sqrt{\omega}}} \left(F(z) - F(0)\right) dz &= -\left(F(z) - F(0)\right) \sqrt{\omega} e^{-\frac{z}{\sqrt{\omega}}} \Big|_0^s - \int_0^s -\sqrt{\omega} e^{-\frac{z}{\sqrt{\omega}}} F'(z)dz \\ &= -\left(F(s) - F(0)\right) \left(\sqrt{\omega} e^{-\frac{s}{\sqrt{\omega}}} \right) + \sqrt{\omega}\left(F(0) - F(0)\right) + \sqrt{\omega} \int_0^s e^{-\frac{z}{\sqrt{\omega}}} e^{\frac{z}{\sqrt{\omega}}} f(u(z))dz \\ &= -\sqrt{\omega} e^{-\frac{s}{\sqrt{\omega}}} \left(F(s) - F(0)\right) + \sqrt{\omega} \int_0^s f(u(z))dz. \end{aligned} \tag{3.17}$$

Plugging in (3.16) into (3.17), we get

$$\begin{aligned} -\sqrt{\omega} e^{-\frac{s}{\sqrt{\omega}}} \int_0^s e^{\frac{t}{\sqrt{\omega}}} f(u(t))dt &+ \sqrt{\omega} \int_0^s f(u(t))dt \\ &= \sqrt{\omega} \int_0^s e^{\frac{s-t}{\sqrt{\omega}}} f(u(t))dt + \int_0^s f(u(t))dt \\ &= \int_0^s \sqrt{\omega} \left(1 - e^{-\frac{s-t}{\sqrt{\omega}}} \right) f(u(t))dt. \end{aligned}$$

Let $G(\mu) = \sqrt{\omega}\left(1 - e^{-\frac{\mu}{\sqrt{\omega}}}\right)$, $\mu > 0$. It follows that

$$\int_0^s \sqrt{\omega}\left(1 - e^{-\frac{s-t}{\sqrt{\omega}}}\right) f(u(t))dt = \int_0^s G(s-t)f(u(t))dt. \tag{3.18}$$

Finally, by plugging in (3.14) and (3.18) into (6.10), we get that

$$u(s) = \frac{1}{2}\alpha^2 + \int_0^s G(s-t)f(u(t))dt = \frac{1}{2}\alpha^2 + \int_0^s G(s-t)\left(1 + D - \sqrt{2u(t)}\right)dt,$$

which concludes the proof. □

3.2 Energy estimate on u

It is necessary for further analysis to prove that solution of equation (3.3) is bounded. To obtain global (independent of s) bounds on u we shall exploit the energy estimate in the way presented in [23].

Theorem 3.2.1. *Solution $u(s)$ of equation (3.3) (or, equivalently, (3.8)) satisfies the following estimate*

$$0 < u(s) < \frac{9}{8}(1 + D)^2, \quad s \geq 0. \tag{3.19}$$

Proof. We will prove the Theorem using the energy estimate. Firstly, multiply (3.3) by u'

$$u'u'' + \frac{1}{\sqrt{\omega}}u'^2 + u'\sqrt{2u} = (1 + D)u'.$$

Notice that

$$\frac{d}{ds}\left(\frac{1}{2}u'^2\right) = u'u'', \quad u'\sqrt{2u} = \frac{d}{ds}\left(\frac{2\sqrt{2}}{3}u^{3/2}\right).$$

It follows that

$$\frac{d}{ds}\left(\frac{1}{2}u'^2 + \frac{2\sqrt{2}}{3}u^{3/2} - (1 + D)u\right) = -\frac{1}{\sqrt{\omega}}u'^2. \tag{3.20}$$

The energy function given by

$$E(s) := \frac{1}{2}u'(s)^2 + \frac{2\sqrt{2}}{3}u(s)^{3/2} - (1 + D)u(s)$$

is nonincreasing since its derivative is nonpositive for all s. Let us compute $E(0)$:

$$E(0) = \frac{1}{2}u'(0)^2 + \frac{2\sqrt{2}}{3}u^{3/2}(0) - (1 + D)u(0) = \frac{2\sqrt{2}}{3}\left(\frac{1}{2}\alpha^2\right)^{3/2} - \frac{1}{2}\alpha^2(1 + D)$$

which leads to

$$E(0) = \frac{1}{3}\alpha^3 - \frac{1}{2}\alpha^2(1 + D) := R(\alpha) \tag{3.21}$$

By our assumption, $0 < H(0) = \alpha << 1$. We want to determine sign of $E(0)$.

$$E(0) = R(\alpha) = \frac{1}{3}\alpha^2 \underbrace{\left(\alpha - \frac{3}{2}(1+D)\right)}_{<0} < 0,$$

for small positive parameter D.

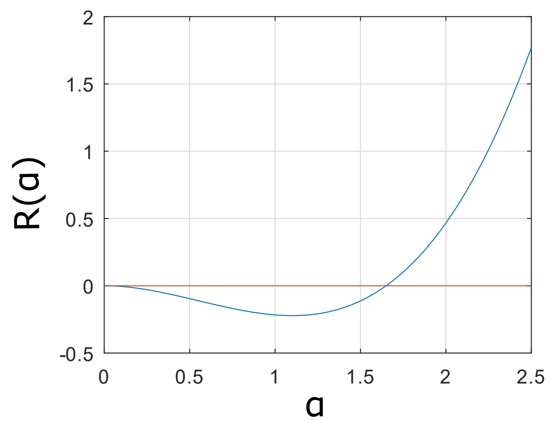

Figure 3.1. Change of the energy function at initial time ($R(\alpha)$) with scaled initial height of a liquid column in a pipe (α). In this case, D = 0.1.

As proven above, $E(0) = R(\alpha)$ will have negative values for all $\alpha \in (0, 1)$. Therefore, function $E(s)$ is nonincreasing and for $s > 0$ we have that

$$E(s) \leq E(0) < 0, \quad \alpha \in (0, 1).$$

It implies that

$$0 > \frac{1}{2}u'(s)^2 + \frac{2\sqrt{2}}{3}u(s)^{3/2} - (1+D)u(s) \geq \frac{2\sqrt{2}}{3}u(s)^{3/2} - (1+D)u(s). \tag{3.22}$$

Last inequality hold since $\frac{1}{2}u'(s)^2 \geq 0$.

By Lemma 3.1.1, $u(s) = \frac{1}{2}H(T)^2$ and therefore $u(s) > 0$ for every $s > 0$. On the other hand, from (3.22) we have that

$$u(s)\left(\frac{2}{3}\sqrt{2u(s)} - (1+D)\right) < 0 \quad \Rightarrow \quad \left(\frac{2}{3}\sqrt{2u(s)} - (1+D)\right) < 0,$$

which implies

$$u(s) < \frac{9}{8}(1+D)^2. \tag{3.23}$$

It follows that

$$0 < u(s) < \frac{9}{8}(1+D)^2,$$

which completes the proof. □

3.3 Existence and uniqueness

Our goal is to apply Banach fixed point theorem in order to show existence and uniqueness of a solution $u(s)$. Energy estimate provided us with upper and lower bound for $u(s)$ under the assumption that it exists. We will introduce an operator $A(u)(s)$ to put equation (3.8) into operator form $A(u)(s) = u(s)$, and show that $A(u)(s)$ is contractive. Beforehand, it is necessary to show that $f(u)$ is Lipschitz continuous.

Lipschitz continuity

Lemma 3.3.1. *For any $v, w \in C([0,S]; \mathbb{R}^+)$ and $D \in \mathbb{R}^+$, function $f(u) = 1 + D - \sqrt{2u}$ is Lipschitz continuous.*

Proof. Taking two arbitrary functions $v, w \in C([0,S]; \mathbb{R}^+)$, we have

$$\begin{aligned}|f(v(t)) - f(w(t))| &= |1 + D - \sqrt{2v(t)} - 1 - D + \sqrt{2w(t)}| \\ &= \sqrt{2}|\sqrt{w(t)} - \sqrt{v(t)}| = \sqrt{2}|\sqrt{v(t)} - \sqrt{w(t)}| \\ &= \sqrt{2}|\sqrt{v(t)} - \sqrt{w(t)}| \cdot \frac{\sqrt{v(t)} + \sqrt{w(t)}}{\sqrt{v(t)} + \sqrt{w(t)}} \\ &= \sqrt{2}\frac{|v(t) - w(t)|}{\sqrt{v(t)} + \sqrt{w(t)}} \\ &\leq \frac{1}{2\sqrt{\epsilon}}|v(t) - w(t)|.\end{aligned}$$

Justification for the last inequality: since $v(t)$ and and $w(t)$ are positive, there exists $\epsilon > 0$, $\kappa > 0$ such that

$$\sqrt{v(t)} + \sqrt{w(t)} \geq \kappa\sqrt{\epsilon} \quad \Rightarrow \quad \frac{1}{\kappa\sqrt{\epsilon}} \geq \frac{1}{\sqrt{v(t)} + \sqrt{w(t)}}.$$

If we choose $\kappa = 2\sqrt{2}$, we get

$$\frac{1}{2\sqrt{\epsilon}} \geq \frac{\sqrt{2}}{\sqrt{v(t)} + \sqrt{w(t)}}.$$

Thus, for $t \in [0, S]$ function $f(u)$ is Lipschitz continuous

$$|f(v(t)) - f(w(t))| \leq \frac{1}{2\sqrt{\epsilon}}|v(t) - w(t)|. \tag{3.24}$$

Note that for the proof of Lipschitz continuity $v(t)$ and $w(t)$ do not have to be the solutions of equation (3.3). □

Operator contraction

In order to show existence and uniqueness of the solution of equation (3.8), we shall apply the Banach fixed point theorem. To that end, we have to put (3.8) into operator form and choose the appropriate space of functions.

We define the operator $A(u)(s)$ as

$$A(u)(s) := \frac{1}{2}\alpha^2 + \int_0^s f(u(t))G(s-t)dt. \tag{3.25}$$

Integral equation (3.8) can now be written in equivalent operator form

$$u(s) = A(u)(s). \tag{3.26}$$

We shall seek the solution of (3.26) in the space of continuous functions $C([0,S];\mathbb{R}^+)$ for some arbitrary $S > 0$. We shall equip this space with Bielecki's norm defined as

$$\|u\|_B := \sup_{s\in[0,S]} |e^{-\gamma s}u(s)|, \quad \gamma > 0. \tag{3.27}$$

It is shown (see Chapter 6) that Bielecki's norm is equivalent to classical supremum norm $\|u\|_\infty$.

Our main goal is to prove that operator $A(u)(s)$ is contractive.

Lemma 3.3.2. *Operator $A(u)(s)$ is contractive in $C([0,S];\mathbb{R}^+)$ with respect to Bielecki's norm.*

Proof. First, we consider $|A(u)(s) - A(v)(s)|$ for $u, v \in C([0,S];\mathbb{R}^+)$

$$\begin{aligned}
\Big|A(u)(s) - A(v)(s)\Big| &= \left|\int_0^s \Big[f(u(t)) - f(v(t))\Big]G(s-t)dt\right| \\
&\le \int_0^s |(f(u(t)) - f(v(t)))|\, G(s-t)dt \\
&= \int_0^s |e^{-\gamma t}(f(u(t)) - f(v(t)))\,|e^{\gamma t}G(s-t)dt \\
&\le \int_0^s \|f(u) - f(v)\|_B e^{\gamma t}G(s-t)dt \\
&= \|f(u) - f(v)\|_B \int_0^s e^{\gamma t}G(s-t)dt.
\end{aligned} \tag{3.28}$$

Next we introduce change of variables

$$\begin{aligned}
s - t = z \quad &\Longrightarrow \quad t = s - z \\
&\qquad\;\; dt = -dz \\
t = 0 \quad &\Longrightarrow \quad z = s \\
t = s \quad &\Longrightarrow \quad z = 0.
\end{aligned}$$

Thus,

$$||f(u) - f(v)||_B \int_s^0 -e^{\gamma(s-z)}G(z)dz = ||f(u) - f(v)||_B e^{\gamma s}\int_0^s e^{-\gamma z}G(z)dz.$$

Multiplying equation (3.28) by $e^{-\gamma s}$ we obtain

$$\Big|A(u)(s) - A(v)(s)\Big|e^{-\gamma s} \le ||f(u) - f(v)||_B e^{\gamma s}e^{-\gamma s}\int_0^s e^{-\gamma z}G(z)dz,$$

that is

$$\left|\left|A(u)(s) - A(v)(s)\right|\right|_B \leq ||f(u) - f(v)||_B \int_0^s e^{-\gamma z} G(z) dz$$
$$\leq \frac{1}{2\sqrt{\epsilon}} ||u - v||_B \left(\int_0^s e^{-\gamma z} G(z) dz \right).$$

Since $\gamma > 0$ is an arbitrary fixed parameter, it can be chosen so that

$$\int_0^s e^{-\gamma z} G(z) dz = 2\sqrt{\epsilon} k,$$

for some $k \in (0, 1)$. This implies

$$\left|\left|A(u)(s) - A(v)(s)\right|\right|_B \leq k\|u - v\|_B, \tag{3.29}$$

which proves that $A(u)(s)$ is contractive. □

We have proved that $Au(s) = u(s)$ is contraction for all $s \in [0, S]$, where S is arbitrary but fixed. From Banach fixed point theorem (see Chapter 6) existence and uniqueness directly follow.

Theorem 3.3.3. *Equation* (3.8) *has unique solution* $u \in C([0, S]; \mathbb{R}^+)$.

Proof. Since (3.8) is equivalent to operator equation (3.26), and operator $A(u)(s)$ is contractive, existence and uniqueness follow from direct application of the Banach fixed point theorem. □

Remark on the applicability of Banach fixed point theorem. Existence and uniqueness are proved above by application of the Banach fixed point theorem on the whole domain. In [23] that was prevented by the loss of Lipschitz continuity of the function $f(u)$, caused by the singular initial condition $u(0) = 0$. In that study global uniqueness was proved by applying Schauder's theorem along with Banach theorem. In our case, problematic initial condition was replaced by $u(0) = \alpha^2/2 > 0$, Lipshitz continuity of function $f(u)$ was regained, and it was possible to extend the applicability of Banach theorem to the whole domain.

3.3.1 Estimates on u

In this section, we estimate the range of $u(s)$ from integral form (3.8) of the governing equation. Since the range depends on s, the domain of its validity wiil be determined as well.

Range

Theorem 3.3.4. *The range of* $u(s)$ *from the equation* (3.8) *is*

$$u(s) \in \left[\frac{1}{2}\alpha^2 + (1 + D - \alpha)\frac{s^2}{2} - (1 + D)\frac{\sqrt{\omega}}{\alpha}\frac{s^3}{6}, \frac{1}{2}\alpha^2 + (1 + D)\frac{s^2}{2} \right].$$

Proof. Let

$$u(s) \geq 0 =: u_0. \tag{3.30}$$

It follows that

$$1 + D - \sqrt{2u} \leq 1 + D,$$

and therefore upper bound is

$$\begin{aligned}
u(s) \leq u_1(s) &:= \frac{1}{2}\alpha^2 + \int_0^s (1+D)G(s-t)dt \\
&= \frac{1}{2}\alpha^2 + (1+D)\int_0^s \sqrt{\omega}\left(1 - e^{-\frac{s-t}{\sqrt{\omega}}}\right)dt \\
&= \frac{1}{2}\alpha^2 + (1+D)\sqrt{\omega}\int_0^s \left(1 - e^{-\frac{s}{\sqrt{\omega}}}\right)dt \\
&= \frac{1}{2}\alpha^2 + \sqrt{\omega}(1+D)\left(s - e^{-\frac{s}{\sqrt{\omega}}}\int_0^s e^{\frac{t}{\sqrt{\omega}}}dt\right) \\
&= \frac{1}{2}\alpha^2 + (1+D)\sqrt{\omega}\left(s - \sqrt{\omega}\left(1 - e^{-\frac{s}{\sqrt{\omega}}}\right)\right) \\
&\leq \frac{1}{2}\alpha^2 + (1+D)s\sqrt{\omega} - (1+D)\omega\left(1 - \left(1 - \frac{s}{\sqrt{\omega}} + \frac{1}{2}\cdot\frac{s^2}{\omega}\right)\right) \\
&= \frac{1}{2}\alpha^2 + \frac{s^2(1+D)}{2}.
\end{aligned}$$

For the proof of inequality, see Chapter 6. Similarly, we estimate the lower bound

$$\begin{aligned}
u(s) \geq u_2(s) &:= \frac{1}{2}\alpha^2 + \int_0^s \left(1 + D - \sqrt{2u_1(t)}\right)G(s-t)dt \\
&\geq \frac{1}{2}\alpha^2 + \int_0^s \left(1 + D - \sqrt{(1+D)t^2 + \alpha^2}\right)G(s-t)dt,
\end{aligned} \tag{3.31}$$

where the last inequality follows from

$$\begin{aligned}
u_1 \leq \frac{1}{2}\alpha^2 + (1+D)\frac{s^2}{2} &\iff 2u_1 \leq (1+D)s^2 + \alpha^2 \\
&\iff \sqrt{2u_1} \leq \sqrt{(1+D)s^2 + \alpha^2} \\
&\iff 1 + D - \sqrt{2u_1} \geq 1 + D - \sqrt{(1+D)s^2 + \alpha^2}.
\end{aligned}$$

Applying last inequality to equation (3.31), we obtain

$$
\begin{aligned}
u(s) &\geq \frac{1}{2}\alpha^2 + \int_0^s \left[1 + D - \alpha - \frac{1}{2}\frac{(1+D)}{\alpha}t^2\right] G(s-t)dt \\
&\geq \frac{1}{2}\alpha^2 + \frac{\sqrt{\omega}}{\alpha}\Bigg[-(1+D)\frac{s^3}{6} + (1+D)\sqrt{\omega}\frac{s^2}{2} \\
&\qquad + \left[(1+D)(\omega-\alpha) + \alpha^2\right] \underbrace{\left(-s + \sqrt{\omega}(1 - e^{-\frac{s}{\sqrt{\omega}}})\right)}_{=:W} \Bigg].
\end{aligned}
$$

Now consider

$$
\begin{aligned}
W &= \left(-s + \sqrt{\omega}(1 - e^{-\frac{s}{\sqrt{\omega}}})\right) = \left(-\sqrt{\omega}\frac{s}{\sqrt{\omega}} + \sqrt{\omega}(1 - e^{-\frac{s}{\sqrt{\omega}}})\right) \\
&= \sqrt{\omega}\left[1 - e^{-\frac{s}{\sqrt{\omega}}} - \frac{s}{\sqrt{\omega}}\right] \\
&\geq \sqrt{\omega}\left[1 - \left(1 - \frac{s}{\sqrt{\omega}} + \frac{1}{2}\frac{s^2}{\omega}\right) - \frac{s}{\sqrt{\omega}}\right] \\
&= \sqrt{\omega}\left(-\frac{1}{2}\frac{s^2}{\omega}\right),
\end{aligned}
$$

where we used $e^{-x} \leq 1 - x + x^2/2$ for $x \geq 0$, which is proved in Chapter 6. Thus,

$$
\begin{aligned}
u(s) &\geq \frac{1}{2}\alpha^2 + \frac{\sqrt{\omega}}{\alpha}\left[-(1+D)\frac{s^3}{6} + (1+D)\sqrt{\omega}\frac{s^2}{2} - \sqrt{\omega}\left[(1+D)(\omega-\alpha) + \alpha^2\right]\frac{s^2}{2\omega}\right] \\
&= \frac{1}{2}\alpha^2 + \frac{1}{2}\left[-(1+D)\sqrt{\omega}\frac{s^3}{6} + \left[(1+D)\omega - (1+D)(\omega-\alpha) - \alpha^2\right]\frac{s^2}{2}\right] \\
&= \frac{1}{2}\alpha^2 + (1+D-\alpha)\frac{s^2}{2} - (1+D)\frac{\sqrt{\omega}}{\alpha}\frac{s^3}{6}.
\end{aligned}
$$

Finally, we obtain

$$
\frac{1}{2}\alpha^2 + (1+D-\alpha)\frac{s^2}{2} - (1+D)\frac{\sqrt{\omega}}{\alpha}\frac{s^3}{6} \leq u(s) \leq \frac{1}{2}\alpha^2 + (1+D)\frac{s^2}{2}. \tag{3.32}
$$

□

Domain

In this section we use previous estimates to determine domain of the solution of (3.3).

Theorem 3.3.5. *The domain of $u(s)$ from the equation (3.8) is* $s \in \left[0, \frac{3\alpha(1+D-\alpha)}{\sqrt{\omega}(1+D)}\right]$.

Proof. From energy estimate, the range of $u(s)$ is

$$0 \leq u(s) \leq \frac{9}{8}(1+D)^2,$$

taking the estimate (3.32) into consideration, it follows that

$$0 \leq \frac{1}{2}\alpha^2 + (1+D-\alpha)\frac{s^2}{2} - (1+D)\frac{\sqrt{\omega}}{\alpha}\frac{s^3}{6} \leq \frac{9}{8}(1+D)^2.$$

We shall focus on the left inequality

$$0 \leq \frac{1}{2}\alpha^2 + \frac{s^2}{2}\left(1+D-\alpha-(1+D)\frac{s\sqrt{\omega}}{3\alpha}\right).$$

Exact upper bound $s_{\max}$ for the variable s is obtained as solution of the cubic equation

$$\frac{1}{2}\alpha^2 + \frac{s^2}{2}\left(1+D-\alpha-(1+D)\frac{s\sqrt{\omega}}{3\alpha}\right) = 0,$$

and it can be shown that it has only one real solution $s > 0$. However, we may obtain considerably simpler estimate on s taking into account that $0 < \alpha^2 \ll 1$, and neglecting the term $\alpha^2/2$

$$0 \leq \frac{s^2}{2}\left(1+D-\alpha-(1+D)\frac{s\sqrt{\omega}}{3\alpha}\right).$$

Therefore,

$$1+D-\alpha-(1+D)\frac{s\sqrt{\omega}}{3\alpha} \geq 0,$$

which implies,

$$s \leq \tilde{s}_{\max} = \frac{3\alpha(1+D-\alpha)}{\sqrt{\omega}(1+D)}.$$

Our final estimate on s, including D, reads:

$$0 \leq s \leq \frac{3\alpha(1+D-\alpha)}{\sqrt{\omega}(1+D)}. \tag{3.33}$$

Note that $\tilde{s}_{\max} < s_{\max}$. □

Chapter 4

Asymptotic and Stability Analysis

In this Chapter we shall focus on quantitative aspects of the Washburn's equation. Namely, equation (2.41) is the most general one that describes capillary flow in our context, but there appear many simplified versions in the literature [34; 9; 24] which are applicable to certain regimes of motion. Since most of these studies introduce simplifications on a phenomenological basis (see [20] for a detailed overview), our aim is to arrive to these simplified models through rigorous asymptotic analysis.

Another aspect of the problem that will be covered is the stability analysis of the stationary solution. In [34; 23] it was shown that the equilibrium height may be approached either monotonically, or oscillatory. This is strongly related to stability properties of the stationary point. Therefore, we shall apply the linear stability analysis to confirm these properties.

Finally, we shall numerically compute the solution of the Washburn's equation to illustrate the results of stability analysis, and to compare it with available experimental data.

4.1 Asymptotic analysis

In this Section we provide new scaling of the equation

$$\omega(HH')' + HH' + H = 1 + D. \tag{4.1}$$

with dimensionless parameter ω

$$\omega = \frac{h_e}{g\tau^2} = \frac{\rho^2 R^4 g}{64\mu^2 h_e}. \tag{4.2}$$

This analysis is motivated by possible further simplifications of equation (4.1) as a consequence of negligible influence of certain physical mechanisms. In particular, one may recognize the following terms in (4.1):

(a) $\omega(HH')'$ – inertial term,

(b) HH' – viscous term,

(c) H – gravity term,

(d) $1 + D$ – capillary term.

Equation (4.1) may be simplified if certain term is much smaller than the others, which are in turn of the same order of magnitude. To that end, new scaling is required becuase (4.1) is only one possible dimensionless (sclaed) form of the governing equation, and cannot comprise all the possibilities.

Let us now introduce the new scaling:

$$h^* = \frac{H}{\hat{h}}, \quad t^* = \frac{T}{\hat{t}},$$

and plug it in equation (4.1) in order to get.

$$\omega \frac{\hat{h}^2}{\hat{t}^2} \frac{d}{dt^*} \left(h^* \frac{dh^*}{dt^*} \right) + \frac{\hat{h}^2}{\hat{t}} h^* \frac{dh^*}{dt^*} + \hat{h} h^* = 1 + D. \tag{4.3}$$

We assume that scaled height and time are power law functions of ω, that is:

$$\hat{h} = \omega^{\beta}, \quad \hat{t} = \omega^{\alpha}.$$

Next, plug these expressions in equation (4.3),

$$\omega^{2\beta+1-2\alpha} (h^* h^{*\prime})' + \omega^{2\beta-\alpha} \cdot h^* h^{*\prime} + \omega^{\beta} h^* = 1 + D. \tag{4.4}$$

Note that capillary term on the right hand side is of order of unity, $1 + D = O(1)$, and cannot be further scaled. Therefore, other terms in (4.4) have to balanced with it. There are three terms on the left hand side and therefore, we discuss three possible cases.

Case 1: Negligible gravity. Capillary forces are balanced by inertial and viscous terms, which are supposed to be of order of unity. In other words, coefficients with inertial and viscous term has to be equal one, that is:

$$2\beta + 1 - 2\alpha = 0,$$
$$2\beta - \alpha = 0,$$

which implies:

$$\alpha = 1, \quad \beta = \frac{1}{2}.$$

Therefore, equation (4.4) becomes

$$(h^* h^{*\prime})' + h^* h^{*\prime} + \omega^{1/2} h^* = 1 + D.$$

Letting $\omega \to 0$ we obtain the simplified equation for the case of negligible gravity term

$$(h^* h^{*\prime})' + h^* h^{*\prime} = 1 + D. \tag{4.5}$$

Case 2: Negligible inertia. Capillary forces are balanced by viscous and gravitational terms. Similarly as in the case above, if a small coefficient is with inertial term, viscous and gravitational terms are of order of unity. It follows that

$$2\beta - \alpha = 0,$$
$$\beta = 0.$$

which implies,

$$\alpha = \beta = 0.$$

This solution transforms equation (4.4) into

$$\omega(h^* h^{*\prime})' + h^* h^{*\prime} + h^* = 1 + D.$$

Letting $\omega \to 0$ we obtain the simplified equation for the case of negligible inertial term

$$h^* h^{*\prime} + h^* = 1 + D. \tag{4.6}$$

Case 3: Negligible viscosity. Capillary forces are balanced by inertial and gravitational terms. If inertial and gravitational terms are of order of unity, it follows that

$$\begin{aligned} 2\beta + 1 - 2\alpha &= 0, \\ \beta &= 0. \end{aligned}$$

which implies,

$$\alpha = \frac{1}{2}, \quad \beta = 0,$$

and reduces equation (4.4) to

$$(h^* h^{*\prime})' + \omega^{-1/2} h^* h^{*\prime} + h^* = 1 + D.$$

It is obvious that viscous term cannot become negligible when $\omega \to 0$. However, it may be neglected for $\omega \to \infty$, leading to the following simplified equation

$$(h^* h^{*\prime})' + h^* = 1 + D. \tag{4.7}$$

Asymptotic analysis presented above relied on the estimate of the dimensionless parameter ω. Equations (4.5) and (4.6) were derived for $\omega \to 0$, which is possible when gravitational acceleration g or density ρ of the fluid are small relative to other terms in (4.2). On the other hand, equation (4.7) is obtained for $\omega \to \infty$, which is possible when viscosity μ of the fluid is small relative to other terms in (4.2).

4.2 Stability analysis of the Washburn's equation

Important part of the analysis of dynamical systems is stability analysis of stationary points. Theoretical background for the stability analysis is provided in Chapter 6.

In the case of Washburn's equation, stability analysis reveals one interesting feature of the terminal part of motion of the liquid column. It approaches asymptotically the stable terminal state (stationary point), but this approach may be either monotonic, or oscillatory. This feature has been analysed in [23] and confirmed in experiments [34; 18].

In the sequel, we shall recover the results of stability analysis presented in [23] and provide the phase space analysis of the Washburn's equation. To that end, we shall consider the equation

$$HH' + H + \omega(HH')' = 1 + D, \tag{4.8}$$

with initial conditions

$$H(0) = \alpha, \quad H'(0) = 0, \tag{4.9}$$

instead of equation (3.3) used in [23].

Theorem 4.2.1. *For equation* (4.8) *the following holds:*

(i) equation (4.8) *has unique stationary point*

$$H_0 = 1 + D; \tag{4.10}$$

(ii) the stationary point (4.10) *is asymptotically stable;*

(iii) parameter ω has a critical value

$$\omega_* = \frac{1+D}{4}; \tag{4.11}$$

for $\omega < \omega_*$ stationary point is stable node; for $\omega > \omega_*$ stationary point is stable focus.

Proof. (i) Consider equation (4.8) and determine the existence of particular (stationary) solution:

$$H(T) = H_0 = \text{const.}, \quad H'(T) = 0 = \text{const.} \tag{4.12}$$

Substituting (4.12) in (4.8) leads to $H_0 = 1 + D$.

(ii) Introduce the change of variables

$$\begin{aligned} H(T) &= x(T), \\ H'(T) &= y(T) \end{aligned}$$

and transform equation (4.8) into a system

$$\begin{aligned} x' &= y, \\ \omega(xy)' + xy &= 1 + D. \end{aligned}$$

We obtain a system of differential equations which is linear with respect to first derivatives:

$$\begin{aligned} x' &= y, \\ \omega\left(x'y + xy'\right) + xy &= 1 + D, \end{aligned}$$

and we may solve it with respect to x' and y':

$$\begin{aligned} x' &= y, \\ y' &= \frac{1}{\omega}\left(\frac{1+D}{x} - y - 1\right) - \frac{y^2}{x}. \end{aligned} \tag{4.13}$$

Defining

$$F_1(x,y) = y, \quad F_2(x,y) = \frac{1}{\omega}\left(\frac{1+D}{x} - y - 1\right) - \frac{y^2}{x},$$

we may rewrite the system (4.13) in the standard form:

$$\begin{aligned} x' &= F_1(x,y), \\ y' &= F_2(x,y), \end{aligned} \tag{4.14}$$

and perform the stability analysis as presented in Chapter 6.

First, we determine the stationary points of (4.14):

$$\begin{aligned} F_1(x_0, y_0) = 0 \quad &\Rightarrow \quad y_0 = 0 \\ F_2(x_0, y_0) = 0 \quad &\Rightarrow \quad x_0 = 1 + D. \end{aligned} \tag{4.15}$$

Notice that stationary point (4.15) is equvalent to stationary solution (4.12) with (4.10), obtained in the proof of (i).

Next, we want to analyze the behavior of the system in the neighborhood of the stationary point (x_0, y_0) determined by (4.15). To that end we introduce the perturbations $\xi(T)$ and $\eta(T)$:

$$\begin{aligned} x = x_0 + \xi = 1 + D + \xi \quad &\Rightarrow \quad x' = \xi', \\ y = y_0 + \eta = \eta \quad &\Rightarrow \quad y' = \eta', \end{aligned}$$

Substituting these results in (4.13), we obtain the variational equations:

$$\begin{aligned} \xi' &= \eta, \\ \eta' &= \frac{1}{\omega}\left(\frac{x_0}{x_0 + \xi} - 1 - \eta\right) - \frac{\eta^2}{x_0 + \xi}, \end{aligned} \tag{4.16}$$

which may be written in standard form:

$$\begin{aligned} \xi' &= F_1(x_0 + \xi, y_0 + \eta), \\ \eta' &= F_2(x_0 + \xi, y_0 + \eta). \end{aligned} \tag{4.17}$$

In the next step we derive the linearised variational equations:

$$\begin{aligned} \xi' &= \frac{\partial F_1(x_0, y_0)}{\partial x}\xi + \frac{\partial F_1(x_0, y_0)}{\partial y}\eta, \\ \eta' &= \frac{\partial F_2(x_0, y_0)}{\partial x}\xi + \frac{\partial F_2(x_0, y_0)}{\partial y}\eta. \end{aligned} \tag{4.18}$$

We have to find partial derivatives in order to determine their explicit form

$$\begin{aligned} \frac{\partial F_1}{\partial x} &= 0 & &\Rightarrow & \frac{\partial F_1(x_0, y_0)}{\partial x} &= 0, \\ \frac{\partial F_1}{\partial y} &= 1 & &\Rightarrow & \frac{\partial F_1(x_0, y_0)}{\partial y} &= 1, \\ \frac{\partial F_2}{\partial x} &= \frac{x_0}{\omega} \cdot \left(-\frac{1}{x^2}\right) + \frac{y^2}{x^2} & &\Rightarrow & \frac{\partial F_2(x_0, y_0)}{\partial x} &= -\frac{1}{\omega x_0}, \\ \frac{\partial F_2}{\partial y} &= -\frac{1}{\omega} - \frac{2y}{x} & &\Rightarrow & \frac{\partial F_2(x_0, y_0)}{\partial y} &= -\frac{1}{\omega}. \end{aligned}$$

Finally, linearised variational equations are:

$$\begin{aligned} \xi' &= \eta, \\ \eta' &= -\frac{1}{\omega x_0}\xi - \frac{1}{\omega}\eta. \end{aligned} \tag{4.19}$$

They can be written in the matrix form:

$$\boldsymbol{\xi}' = \mathbf{A}\boldsymbol{\xi}, \quad \boldsymbol{\xi} = \begin{bmatrix} \xi \\ \eta \end{bmatrix}, \quad \mathbf{A} = \begin{bmatrix} 0 & 1 \\ -\frac{1}{\omega x_0} & -\frac{1}{\omega} \end{bmatrix}.$$

stability of the stationary point is determined by the eigenvalues of the matrix $\mathbf{A}$, obtained as solutions of the characteristic equation $\det(\mathbf{A} - \lambda\mathbf{I}) = 0$; identity matrix is denoted by $\mathbf{I}$. We have

$$\mathbf{A} - \lambda\mathbf{I} = \begin{bmatrix} -\lambda & 1 \\ -\frac{1}{\omega x_0} & -\frac{1}{w} - \lambda \end{bmatrix},$$

so that

$$\det(\mathbf{A} - \lambda\mathbf{I}) = \lambda\left(\frac{1}{\omega} + \lambda\right) + \frac{1}{\omega x_0} = 0.$$

After minor changes we arrive at quadratic equation

$$\lambda^2 + \frac{1}{\omega}\lambda + \frac{1}{\omega x_0} = 0,$$

whose solutions are

$$\lambda_{1,2} = \frac{-\frac{1}{\omega} \pm \sqrt{\frac{1}{\omega^2} - \frac{4}{\omega x_0}}}{2} = \frac{-\frac{1}{\omega} \pm \sqrt{\frac{1}{\omega^2} - \frac{4\omega}{\omega^2 x_0}}}{2} = \frac{-1 \pm \sqrt{1 - \frac{4\omega}{x_0}}}{2\omega}. \tag{4.20}$$

Discriminant K is given by

$$K = 1 - \frac{4\omega}{x_0} = 1 - \frac{4\omega}{1+D}.$$

Since ω and D are positive, $-\frac{4\omega}{1+D} < 0$ and therefore

$$1 - \frac{4\omega}{1+D} < 1.$$

It follows that both eigenvalues λ_1 and λ_2 have negative real parts for any value of the parameters ω and D. Therefore, the stationary point (x_0, y_0) is **asymptotically stable**.

(iii) Critical value for ω is obtained when discriminant equals zero, i.e.

$$1 - \frac{4\omega}{x_0} = 0 \quad \Rightarrow \quad \omega_* = \frac{x_0}{4} = \frac{1+D}{4}. \tag{4.21}$$

The character of critical point is determined by discussing sign of the discriminant:

- for $\omega < \omega_*$ $(0 < K < 1)$, both eigenvalues are real and negative, $\lambda_2 < \lambda_1 < 0$, and the critical point is **stable node**;
- for $\omega > \omega_*$ $(K < 0)$, eigenvalues are complex conjugate, $\bar{\lambda}_2 = \lambda_1$, with negative real parts, $\mathrm{Re}(\lambda_1) = \mathrm{Re}(\lambda_2) < 0$; therefore, the critical point is **stable focus**.

□

Note that in [23] there is no immersial depth, $D = 0$, so the only difference is in actual critical value ω_*. However, it does not effect the type of the critical point.

4.3 Numerical results

In this Section we show the results of numerical solution of the Washburn's equation, both in the time domain and in the phase plane. Also, we validate the model by comparison with experimental data.

Numerical solutions and phase portraits

We firstly present numerical solutions for test values of the parameter ω in order to confirm the results of stability analysis.

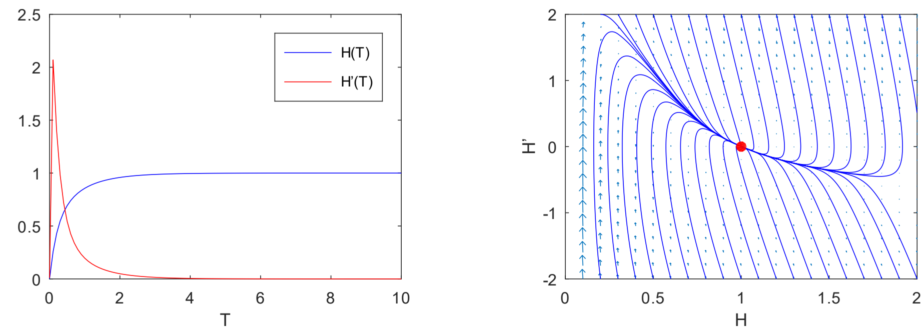

(a) Dimensionless height(blue) and velocity (red) with respect to dimensionless time

(b) Phase portrait - stable node

Figure 4.1. Stability analysis for immersion depth $D = 0$ and $\omega = 0.1$.

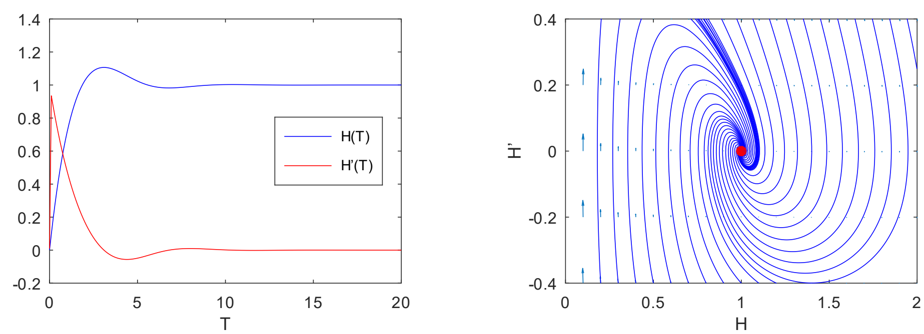

(a) Dimensionless height(blue) and velocity (red) with respect to dimensionless time

(b) Phase portrait - stable focus

Figure 4.2. Stability analysis for immersion depth $D = 0$ and $\omega = 1$.

In Figures 4.1 and 4.2 numerical solutions are presented for $\omega = 0.1$ and $\omega = 1$, respectively. In every case immersion depth is set to $D = 0$. Graphs on the left show dimensionless height $H(T)$ and velocity $H'(T)$ versus dimensionless time T. For $\omega = 0.1 < \dfrac{1}{4}$, the equilibrium point is approached monotonically, while for $\omega = 1 > \frac{1}{4}$ we have oscillatory behaviour. Figures on the right ilustrate phase portraits and it is clear that for $\omega < \frac{1}{4}$ the equilibrium value is stable node, whereas $\omega > \frac{1}{4}$ demonstrates stable focus.

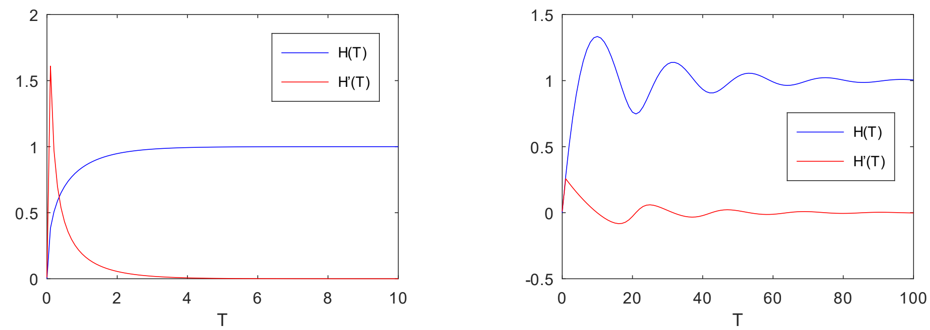

(a) Dodecane, $\omega = 7.8 \cdot 10^{-5}$ (b) Dyethil ether, $\omega = 11.602$

Figure 4.3. Dimensionless height(blue) and velocity (red) with respect to dimensionless time, experimental values from [34]

Different behaviour of the solution for the different values of ω is not only a theoretical result. There are liquids whose physical properties yield the value of ω in either part of the domain. In [34] two liquids were considered, dodecane whose value of the parameter was $\omega \approx 7.8 \cdot 10^{-5}$, and dyethil ether with $\omega \approx 11.602$. Dodecane monotonically approaches equilibrium value, that is stable node. On the other hand, dyethil ether oscillatory approaches equilibrium value, a stable focus. This is shown on Figure 4.3.

Model validation

In this part, we validate our model by comparing to experimental results given in [34]. The liquid considered in the experiment was dodecane, with following parameters $\mu = 1.7 \cdot 10^{-3}$[Pas], $\rho = 750$[kgm^{-3}], $\gamma = 2.5 \cdot 10^{-2}$[Nm^{-1}], $\theta = 17°$, $R = 10^{-4}$[m]. For these values of parameters we have $\omega \approx 4.59 \cdot 10^{-5}$. Column height and time from experiment were casted into dimenionless form with the following scale (2.38)

$$H = \frac{\tilde{h}}{h_e}, \quad T = \frac{t}{\tau},$$

with

$$h_e = \frac{2\gamma \cos(\theta)}{\rho g R}, \qquad \tau = \frac{8\mu h_e}{R^2 \rho g}.$$

In the literature [23; 34] there is a discussion about the initial conditions and the singularity which appears at $T = 0$, which was analyzed in Chapter 2. Since most of the studies use the initial condition $H(0) = 0$, we decided to mimic this situation as much as possible. Therefore, numerical solution was computed for the initial condition $\alpha = 0.001$.

From the results of numerical computation, shown in Figure 4.4, it may be observed that our model yields excellent agreement with experimental data for $T > 0.025$. There appears discrepancy in the initial phase, $0 < T < 0.025$. In [34] this discrepancy was resolved by introduction of an

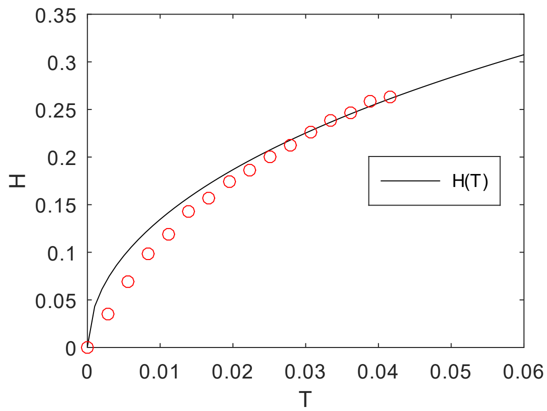

Figure 4.4. Short-time limit of capillary rise. Height of the liquid column(black) compared with experimental values from [34] (red circles).

additional term in the model which describes the turbulent drag. That was motivated by the fact that singular intial condition $H(0) = 0$ yields extremely high initial velocity. In our opinion, these conditions make the assumption of incompressibility questionable. Therefore, possible solution to this problem is to analyse the flow of a compressible fluid in the initial phase.

Chapter 5

Conclusion

Mathematical model of capillary rise in the vascular tissue of plants is provided in this work. In order to give an appropriate theoretical model, we first familiarised ourselves with water transport mechanisms in plants.

Firstly, we have studied properties of vascular tissue (xylem) and provided overview of Cohesion Tension Theory. Cohesion Tension Theory suggests that water rise occurs due to differences in pressure gradient. Moreover, we analysed physical properties of water, which were taken into consideration in the model.

The literature suggested that Washburn's equation describes capillary uptake of fluid and it was derived by applying the Newton's Law of Motion to a control volume. Our idea was to try a different approach, i.e. to derive Washburn's equation using the fundamental equations from continuum mechanics. In this work we gave an overview of mass and momentum balance laws, both in local and global form. Since the conducting element was supposed to be modelled as a pipe, our next task was to present system of equation that describe motion of a fluid (Navier-Stokes equations) in polar cylindrical coordinates.

Derivation of Washburn's equation was split into two parts - local and global analysis. Theoretical assumptions were provided as a part of local analysis. In a global analysis, all the assumptions were taken into consideration, and Washburn's equation is obtained by applying a momentum balance law in global form.

Secondly, our aim was to solve Washburn's equation with general initial conditions. In order to simplify the procedure and reduce it to one parameter, we transformed the equation into dimensionless form. We used energy estimate to show that solution must be always positive. In order to formally prove existence and uniqueness by Banach Contraction Principle, we needed to provide appropriate operator form of the governing equation. After succesfully proving existence and uniqueness of a solution, we determined domain and range of a solution.

Next, we used scaled form of the Washburn's equation to analyse certain asimptotic regimes. In other words, we discussed under which conditions appropriate terms in the equation may be cancelled out. Additionally, stability analysis was conducted. We determined the stationary point and showed that liquid column can approach the stable stationary state either monotonically or oscillatory. Finally, numerical analysis with real experimental data is compared with our model and high compatibility is observed.

Chapter 6

Appendix

6.1 Foundations of Functional Analysis

In this chapter we state foundations of Functional analysis as presented in [33].

Definition 6.1.1. A linear space X over $\mathbb{K}$ is a set X together with an addition

$$u + v, \quad u, v \in X$$

and a scalar multiplication

$$\alpha u, \quad \alpha \in \mathbb{K}, u \in X,$$

where all the usual rules are satisfied.

Definition 6.1.2. Linear space X over $\mathbb{K}$ is called the normed space if there exists a norm $||\cdot|| : X \to \mathbb{R}^+ \cup \{0\}$, such that for all $u, v \in X$ and $\alpha \in \mathbb{K}$, the following are true:

1. $||u|| \geq 0$ (i.e., $||u||$ is a nonnegative real number).
2. $||u|| = 0$ if and only if $u = 0$.
3. $||\alpha u|| = |\alpha| ||u||$.
4. $||u + v|| \leq ||u|| + ||v||$ (triangle inequality).

Definition 6.1.3. Let (u_n) be a sequence in the normed space X, i.e., $u_n \in X$ for all n. We write

$$\lim_{n\to\infty} u_n = u \iff \lim_{n\to\infty} ||u_n - u|| = 0,$$

and we say that the sequence (u_n) converges to u.

Definition 6.1.4. The sequence (u_n) in the normed space X is called a Cauchy sequence iff for each $\epsilon > 0$ there is a number $n_0(\epsilon)$ such that $||u_n - u_m|| < \epsilon$ for all $n, m \geq n_0(\epsilon)$.

Proposition 6.1.0.1. In a normed space, each convergent sequence is Cauchy.

Definition 6.1.5. The normed space X is a Banach space if and only if each Cauchy sequence is convergent.

Definition 6.1.6. Let X be a normed space. For fixed $u_0 \in X$ and $\epsilon > 0$, the set

$$U_\epsilon(u_0) := \{u \in X : ||u - u_0|| < \epsilon\}$$

is called an ϵ-neighbourhood of the point u_0.
The subset M of X is called open iff for each point $u_0 \in M$, there is some ϵ-neighbourhood of the point $U_\epsilon(u_0)$ such that

$$U_\epsilon(u_0) \subseteq M.$$

The subset M of X is closed if and only if its complement is open.

Proposition 6.1.0.2. Let $M \subseteq X$, where X is a normed space. Then the following are equivalent:

- M is closed
- It follows from $u_n \in M$ for all n and $u_n \to u$ as $n \to \infty$, that $u \in M$.

Definition 6.1.7. Let M and Y be sets. An operator

$$A : M \to Y$$

associates to each point u in M a point v denoted by $v = Au$.

Definition 6.1.8. Let M be a set in a normed space.

- M is relatively sequentially compact if and only if each sequence (u_n) in M has a convergent subsequence $u'_n \to u$ as $n' \to \infty$.
- M is sequentially compact if and only if each sequence (u_n) has a convergent subsequence $u'_n \to u$ as $n' \to \infty$ such that $u \in M$.
- M is bounded if and only if there is a number $r \geq 0$ such that $||u|| \leq r$ for all $u \in M$.

Proposition 6.1.0.3. The set M is compact if and only if it is relatively compact and closed.

Definition 6.1.9. Let X and Y be normed spaces over $\mathbb{K}$. The operator is sequentially continuous if and only if, for each sequence (u_n) in M,

$$\lim_{n\to\infty} = u, \ u \in M \quad \Rightarrow \quad \lim_{n\to\infty} Au_n = Au.$$

The operator A is called continuous if and only if for each point $u \in M$ and each number $\epsilon > 0$, there is a number $\delta(\epsilon, u) > 0$ such that

$$||v - u|| < \delta(\epsilon, u), \in M \quad \Rightarrow ||Av - Au|| < \epsilon.$$

In addition, if it is possible to choose the number $\delta(\epsilon, u) > 0$ in such a way that it does not depend on the point $u \in M$, then the operator A is uniformly continuous.

Proposition 6.1.0.4. We are given the operator $A : M \subseteq X \to Y$, where X and Y are normed spaces over $\mathbb{K}$. Then the following two statements are equivalent:

- A is continuous.

- A is sequentially continuous.

Definition 6.1.10. Let X and Y be normed spaces over $\mathbb{K}$. The operator

$$A : M \subseteq X \to Y$$

is compact if and only if

- A is continuos, and
- A transforms bounded sets into relatively compact sets.

The second property is equivalent to the following: If (u_n) is a bounded sequence is M, then there exists a subsequence (u'_n) of (u_n) such that the sequence (Au'_n) is convergent in Y.

Definition 6.1.11. Let X and Y be normed spaces over $\mathbb{K}$. The operator $A : M \subseteq X \to Y$ is called Lipschitz continuous if and only if there is a number $L > 0$ such that

$$||Av - Au|| \leq L||v - u||, \quad for \quad all \quad u, v \in M.$$

Each Lipschitz continuous operator is uniformly continuous.

Definition 6.1.12. The set M in a linear space is convex if and only if

$$u, v \in M, \quad \text{and} \quad 0 \leq \alpha \leq 1 \Rightarrow \alpha u + (1 - \alpha)v \in M.$$

We want to solve the operator equation:

$$u = Au, \quad u \in M, \tag{6.1}$$

by means of the following iteration method:

$$u_{n+1} = Au_n, \quad n = 0, 1, \ldots, \tag{6.2}$$

where $u_0 \in M$. Each solution of (6.1) is called a fixed point of the operator A.

Theorem 6.1.1 (Banach fixed point theorem)**.** *We assume that:*

- *M is a closed nonempty set in the Banach space X over K, and*
- *the operator $A : M \to M$ is k-contractive, i.e. by definition*

  $$||Au - Av|| \leq k||u - v|| \quad for \quad all \quad u, v \in M$$

  and fixed k, $0 \leq k < 1$. Then, the following hold true:

- *Existence and uniqueness. The original equation (6.1) has exactly one solution u, i.e. the operator A has exactly one point u on the set M.*
- *Convergence of the iteration method. For each given $u_0 \in M$, the sequence (u_n) constructed by (6.2) converges to the unique solution u of equation (6.1).*

- *Error estimates. For all $n = 0, 1, \ldots$ we have the a priori estimate*

$$||u_n - u|| \leq \frac{k^n}{k-1}||u_1 - u_0||,$$

and the a posteriori error estimate

$$||u_{n+1} - u|| \leq \frac{k}{k-1}||u_{n+1} - u_n||.$$

- *Rate of convergence. For all $n = 0, 1, \ldots$ we have*

$$||u_{n+1} - u|| \leq k||u_n - u||.$$

6.1.1 Equivalent norms

Definition 6.1.13. Let X be an N-dimensional linear space over K, where $N = 1, 2, \ldots$ By a basis $\{e_1, \ldots, e_N\}$ of X we understand a set of elements $e_1, \ldots, e_N$ of X such that, for each $u \in X$

$$u = \alpha_1 e_1 + \cdots + \alpha_N a_N$$

where the numbers $\alpha_1, \ldots, \alpha_N \in \mathbb{K}$ are uniquely determined by u. The numbers $\alpha_1, \ldots, \alpha_N$ are called the components of u.

Proposition 6.1.1.1. Let $N = 1, 2, \ldots$. In each N-dimensional linear space X over $\mathbb{K}$ there exists a basis $\{e_1, \ldots e_N\}$.

Definition 6.1.14. The two norms $|| \cdot ||$ and $|| \cdot ||_1$ on the normed space X are equivalent if and only if there are positive numbers α and β such that

$$\alpha||u|| \leq ||u||_1 \leq \beta||u|| \quad \text{for all} \quad u \in X.$$

Proposition 6.1.1.2. Two norms on a finite-dimensional linear space X over $\mathbb{K}$ are always equivalent.

Definition 6.1.15. Bielecki's norm of function $u(s)$ is defined as

$$\|u(s)\|_B := \sup_{s \in [0,S]} |e^{-\gamma s} u(s)|, \quad \gamma > 0, S > 0.$$

In the sequel we will need the fact that Bielecki's norm and supremum norm are equivalent on $C([0, S], \mathbb{R}^+)$.

Theorem 6.1.2. *Bielecki's norm and supremum norm of $u(s)$ are equivalent on $[0, \infty)$.*

Proof. Supremum norm of $u(s)$ is defined as

$$\|u\|_\infty \sup_{s \in [0,S]} |u|.$$

We will bound $|e^{-\gamma s} u(s)|$.

$$|e^{-\gamma s} u(s)| = e^{-\gamma s} |u(s)| \leq |u(s)|.$$

Taking supremum on both sides

$$\sup_{s\in[0,S]} |e^{-\gamma s}u(s)| \leq \sup_{s\in[0,S]} |u(s)|,$$

that is,

$$\|u\|_B \leq \|u\|_\infty. \tag{6.3}$$

On the other hand, for $s \in [0, S]$ it follows that $e^{-\alpha s} \geq e^{-\alpha S}$.

$$|e^{-\gamma s}u(s)| = e^{-\gamma s}|u(s)| \geq e^{-\gamma S}|u(s)|.$$

Taking supremum on both sides

$$\sup_{s\in[0,S]} |e^{-\gamma s}u(s)| \geq e^{-\gamma S} \sup_{s\in[0,S]} |u(s)|,$$

which gives

$$\|u\|_B \geq e^{-\gamma S}\|u\|_\infty. \tag{6.4}$$

Combining (6.3) and (6.4), we obtain

$$e^{-\gamma S}\|u\|_\infty \leq \|u\|_B \leq \|u\|_\infty, \tag{6.5}$$

which implies equivalence of these norms. □

In order to apply Banach fixed point theorem we need a closed subset $M \subset C([0, S], \mathbb{R}^+)$.

Lemma 6.1.3. *Set M defined as*

$$M = \left\{ u \in C([0, S], \mathbb{R}^+) : \|u\|_B \leq \frac{9}{8}(1 + D)^2,\ D > 0 \right\}$$

is closed.

Proof. Suppose that $\{u_n\} \subset M$ and $u_n \to g$ in $C([0, S], \mathbb{R}^+)$. We claim that $\|g\|_B \leq \frac{9}{8}(1 + D)^2$. Suppose not, $\|g\|_B > \frac{9}{8}(1 + D)^2$. Let $\delta = \|g\|_B - \frac{9}{8}(1 + D)^2$, that is

$$\|g\|_B = \delta + \frac{9}{8}(1 + D)^2. \tag{6.6}$$

Then there is N such that for $n \geq N$,

$$\|u_n - g\| \leq \frac{\delta}{2}.$$

By the triangle inequality

$$\|g\|_B = \|g - u_n + u_n\|_B \leq \|g - u_n\|_B + \|u_n\|_B \leq \frac{\delta}{2} + \frac{9}{8}(1 + D)^2.$$

It is contradiction with (6.6). Hence, M is closed. □

6.2 Inequalities with series

Theorem 6.2.1 (Mean value theorem)**.** *If f is a continuous function on the closed interval $[a,b]$ and differentiable on the open interval (a,b), then there exist a point c in (a,b) such that*

$$f(b) - f(a) = f'(c)(b-a).$$

Lemma 6.2.2. *For $x > 0$ it holds that*

$$\sqrt{1+x} < 1 + \frac{x}{2}.$$

Proof. If $x > 0$ we apply Mean Value Theorem to $f(x) = \sqrt{1+x}$ on the interval $[0,x]$. There exist $c \in [0,x]$ such that

$$\frac{\sqrt{1+x}-1}{x} = \frac{f(x)-f(0)}{x} = f'(c) = \frac{1}{2\sqrt{1+c}} < \frac{1}{2}.$$

The last inequality holds because $c > 0$. Multiplying the obtained inequality by positive number x gives

$$\sqrt{1+x} < 1 + \frac{x}{2}.$$

□

Theorem 6.2.3 (Taylor's theorem)**.** *Let $f : \mathbb{R} \to \mathbb{R}$ be $k+1$-times differentiable with all derivatives continuous. Fix x_0 and let*

$$P_k(x) = f(x_0) + f'(x_0)(x-x_0) + \cdots + \frac{f^k(x_0)}{k!}(x-x_0)^k$$
$$R_k(\xi;x) = \frac{f^{(k+1)}(\xi)}{(k+1)!}(x-x_0)^{k+1}.$$

Then

$$f(x) = P_k(x) + R_k(\xi;x)$$

for some $\xi \in (x_0,x)$. Note that P_k is interpreted as approximation to f, while $R_k(\xi;x)$ is interpreted as remainder.

Corollary 6.2.3.1. If $R_k(\xi;x) \leq 0$ for all $\xi \in (x_0,x)$, then $f(x) \leq P_k(x)$. Similarly, if $R_k(\xi;x) \geq 0$ for all $\xi \in (x_0,x)$, then $f(x) \geq P_k(x)$.

We were considering the function

$$e^{-x} = \underbrace{\sum_{i=0}^{k} \frac{(-x)^i}{i!}}_{P_k(x)} + \underbrace{(-1)^{k+1}\frac{e^{-x\xi}x^{k+1}}{(k+1)!}}_{R_k(\xi;x)}$$

- Even k:

$$R_k \leq 0 \implies e^{-x} \leq \sum_{i=0}^{k} \frac{(-x)^i}{i!}.$$

- Odd k:

$$R_k \geq 0 \implies e^{-x} \geq \sum_{i=0}^{k} \frac{(-x)^i}{i!}.$$

Thus,

$$1 - x + \frac{1}{2}x^2 - \frac{1}{6}x^3 \leq e^{-x} \leq 1 - x + \frac{1}{2}x^2.$$

6.3 Foundations of stability analysis

Theory of stability is concerned with qualitative properties of solutions of differential equations which are subject to perturbations. We shall present necessary definitions and results related to stability analysis of stationary solutions of autonomous differential systems, as given in [7] and [10].

Definition of stability

Consider the system of differential equations

$$\frac{d\boldsymbol{x}}{dt} = \mathbf{F}(\boldsymbol{x}), \quad \boldsymbol{x} \in \mathbb{R}^n. \tag{6.7}$$

The system (6.7) is to be autonomous since the right hand side does not depend on independent variable t, usually considered to be time variable.

Definition 6.3.1. A point $\boldsymbol{X} \in \mathbb{R}^n$ is said to be the stationary or equilibrium point of the system (6.7) if $\mathbf{F}(\boldsymbol{X}) = \mathbf{0}$.

Lemma 6.3.1. *If $\boldsymbol{X} \in \mathbb{R}^n$ is a stationary point of the system* (6.7)*, then $\boldsymbol{x}(t) = \boldsymbol{X}$ is its particular solution, called stationary or equilibrium solution.*

Consider a solution $\boldsymbol{x}(t)$, $t > 0$, of the system (6.7) for initial conditions $\boldsymbol{x}(0) = \boldsymbol{x}_0$. We now give the definitions of stability in the sense of Lyapunov.

Definition 6.3.2. Let $\boldsymbol{X} \in \mathbb{R}^n$ be a stationary point of the system (6.7).

(i) $\boldsymbol{X}$ is said to be **stable** if for all $\varepsilon > 0$ there exists $\delta(\varepsilon) > 0$, such that

$$\|\boldsymbol{x}(t) - \boldsymbol{X}\| < \epsilon,$$

for every $\boldsymbol{x}_0$ which satisfies $\|\boldsymbol{x}_0 - \boldsymbol{X}\| < \delta(\varepsilon)$.

(ii) $\boldsymbol{X}$ is said to be **asymptotically stable** if it is stable and moreover

$$\lim_{t \to \infty} \boldsymbol{x}(t) = \boldsymbol{X}.$$

Stability of the stationary point, in the sense defined above, is considered to be a local property since it is assumed that ε is small. Therefore, it is usually regarded as stability with respect to small perturbations in initial conditions. Definition given above deals with stability of the stationary point, but it can be easily generalized to stability of any particular solution of the system (6.7), see [10].

There are several methods/criteria for detrmination whether a stationary point is stable [7; 27]. In the sequel we shall focus on linear stability analysis of stationary points for second-order systems. In this case it is possible to provide detailed characterization of the stationary points based upon local behaviour of the solutions.

Second-order autonomous differential systems

An important class of systems of ordinary differential equations is that of second-order autonomous systems,

$$\frac{d\boldsymbol{x}}{dt} = \mathbf{F}(\boldsymbol{x}), \tag{6.8}$$

where, $\boldsymbol{x} = [x, y]^T$ and $\mathbf{F}(\boldsymbol{x}) = [F(x, y), G(x, y)]^T$. This can be written in component form:

$$\frac{dx}{dt} = F(x, y), \quad \frac{dy}{dt} = G(x, y). \tag{6.9}$$

Properties are investigated both by analytical and geometrical methods. The phase plane is used for examining orbits in the (x, y)-plane, the curves with the equation

$$\frac{dy}{dx} = \frac{G(x, y)}{F(x, y)}.$$

Classification of equilibrium points is determined by the local behaviour of orbits.

Suppose that the system (6.8) has a point $\boldsymbol{X}$ of equilibrium, such that $\mathbf{F}(\boldsymbol{X}) = \mathbf{0}$, where $\boldsymbol{X} = [X, Y]^T$. Without loss of generality we may translate the equilibrium point to the origin so that $\boldsymbol{X} = \mathbf{0}$. Then $F(0, 0) = G(0, 0) = 0$. To consider orbits of (6.8) near $\mathbf{0}$, assume that $\mathbf{F}$ is continuously twice differentiable, so

$$\begin{aligned} F(x, y) &= ax + by + O(x^2 + y^2), \\ G(x, y) &= cx + dy + O(x^2 + y^2) \quad x, y \to 0, \end{aligned}$$

where $a = [\partial F/\partial x]_0$, $b = [\partial F/\partial y]_0$, $c = [\partial G/\partial x]_0$, and $d = [\partial G/\partial y]_0$. Then the behaviour of the system (6.8) may in general be approximated locally by the linearised system

$$\frac{d\boldsymbol{x}}{dt} = \mathbf{J}\boldsymbol{x}, \tag{6.10}$$

where the column vector $\boldsymbol{x} = [x, y]^T$ and the 2×2 matrix

$$\mathbf{J} = \begin{bmatrix} a & b \\ c & d \end{bmatrix}.$$

Equilibrium points of the system (6.10) are analysed according to properties of $\mathbf{J}$.

The linear system (6.10) with constant coefficients can be solved, in general, by seeking solutions $\boldsymbol{x}(t) = e^{st}\boldsymbol{u}$, for a constant vector $\boldsymbol{u}$. Then

$$\mathbf{J}\boldsymbol{u} = s\boldsymbol{u},$$

i.e. s is the eigenvalue of $\mathbf{J}$ and $\boldsymbol{u}$ is the corresponding eigenvector. Therefore,

$$\begin{aligned} 0 &= \begin{vmatrix} a - s & b \\ c & d - s \end{vmatrix} \\ &= s^2 - ps + q, \end{aligned} \tag{6.11}$$

where $p = \text{tr}(\mathbf{J}) = a + d$ and $q = \det(\mathbf{J})$. Therefore, $s = s_1$ or s_2, where

$$s_1, s_2 = \frac{1}{2}\{p \pm \sqrt{(p^2 - 4q)}\}.$$

Therefore, if $p^2 \neq 4q$, the general solution of (6.10) is

$$\boldsymbol{x}(t) = C_1 e^{s_1 t}[u_1, v_1]^T + C_2 e^{s_2 t}[u_2, v_2]^T \tag{6.12}$$

for arbitrary constants C_1 and C_2, where the eigenvalue s_j belongs to eigenvector $\boldsymbol{u}_j = [u_j, v_j]^T$ for $j = 1, 2, ...$ where

$$au_j + bv_j = s_j u_j, \quad cu_j + dv_j = s_j v_j.$$

The explicit solution, and the solution for the case $p^2 = 4q$ of a double eigenvalue, enable us to classify all the equilibrium points as follows:

1. **Node:** $p^2 > 4q$ and $q > 0$. Here s_1, s_2 are real, distinct and of the same sign. We take $s_1 > s_2$ without loss of generality. Therefore,

$$x(t) \sim C_1 e^{s_1 t}[u_1, v_1]^T \quad as \quad t \to \infty$$

if $C_1 \neq 0$, and so

$$\frac{y}{x} \to \frac{v_1}{u_1} \quad as \quad t \to \infty$$

This describes a node, which is stable if $s_1 < 0$ and so if $p < 0$ and unstable if $p > 0$.

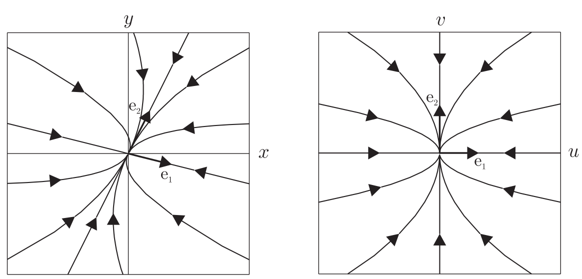

(a)

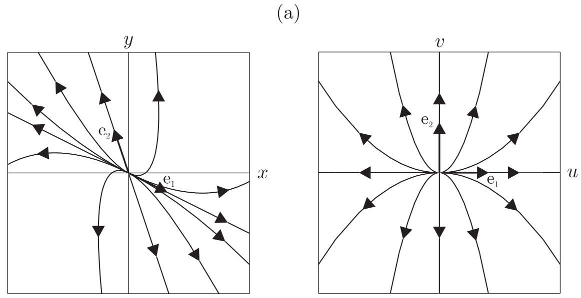

(b)

Figure 6.1. Phase portrait of linear sistem in the neighbourhood of (a) stable and (b) unstable node. [27]

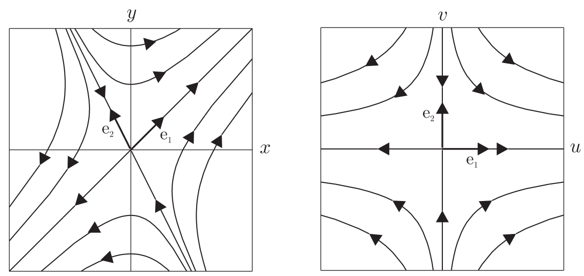

Figure 6.2. Phase portrait of linear sistem in the neighbourhood of saddle. [27]

2. **Saddle point**: $p^2 > 4q$ and $q < 0$. Here s_1, s_2 are real and of opposite signs, so we may take $s_1 > 0 > s_2$ without loss of generality. The orbits near $\mathbf{0}$ resemble hyperbolae.

3. **Focus:** $p^2 < 4q$ and $p \neq 0$. Here s_1 and s_2 are a complex conjugate pair with non-zero real part, so we may take $s_1 = \overline{s_2} = \frac{1}{2}\{p + i\sqrt{(4q - p^2)}\}$. Then,

$$\boldsymbol{x}(t) = Ce^{\frac{pt}{2}} \left[\cos\left(\beta t + \gamma\right), K\cos\left(\beta t + \gamma + \delta\right)\right]^T$$

where C, γ are arbitrary real constants, $\beta = \sqrt{q - \frac{p^2}{4}}$ and K, δ are real constants determined by a, b, c and d. Therefore, the origin is a stable point of equilibrium if $p < 0$ and unstable if $p > 0$. These are typical cases for which no two eigenvalues are equal and the real part of no eigenvalue iz zero.There are a few special cases that remain to be described.

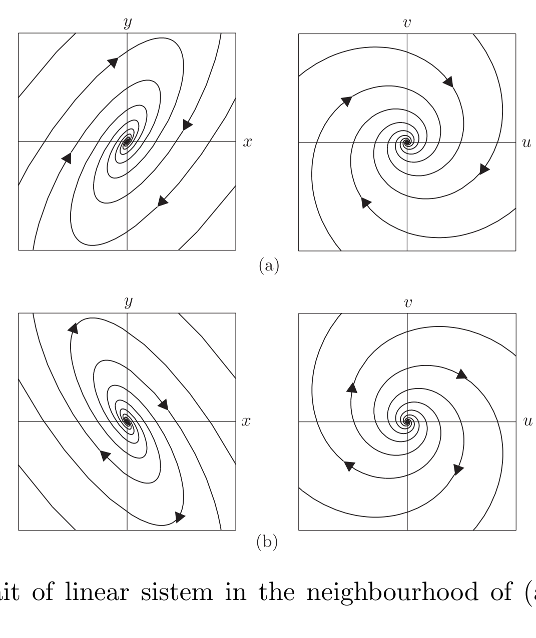

Figure 6.3. Phase portrait of linear sistem in the neighbourhood of (a) stable and (b) unstable focus. [27]

4. **Improper node:** $p^2 = 4q$ and $q > 0$. Here $s_1 = s_2$ is real. The solution can in general to be shown to give a limiting form of a node because the lines $y = v_1x/u_1$ and $y = v_2x/u_2$ coincide. The node is stable if $p < 0$ and unstable if $p > 0$.

5. **Centre:** $p^2 < 4q$ and $p = 0$, i.e. $p = 0$ and $q > 0$. Here $s_1, s_2 = \pm i\sqrt{q}$ are purely imaginary. Then

$$\boldsymbol{x}(t) = [C\cos(t\sqrt{q} + \gamma), K\cos(t\sqrt{q} + \gamma + \delta)]^T$$

where C, γ are arbitrary real constants and K, δ are real constants determined by a, b, c and d. The orbits are ellipses with centre at the origin.

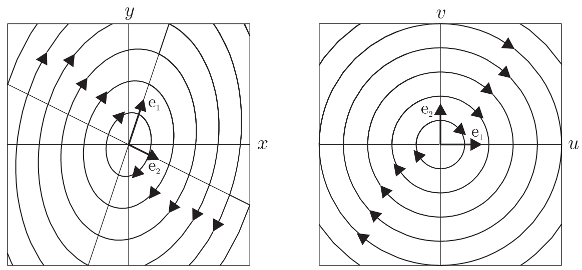

Figure 6.4. Phase portrait of linear sistem in the neighbourhood of centre. [27]

6. **Degenerate node:** $p^2 > 4q$ and $q = 0$, i.e. $p^2 > 0$ and $q = 0$. This is the limiting case of 1) above, for which we may put $s_1 = 0$ and $s_2 = p$. Therefore,

$$\boldsymbol{x}(t) = C_1[u_1, v_1]^T + C_2e^{pt}[u_2, v_2]^T$$

and the orbits are straight lines parallel to $y = v_2x/u_2$, approaching the line $y = u_1x/v_1$ as $t \to \infty$ if $p < 0$ and leaving it if $p > 0$.

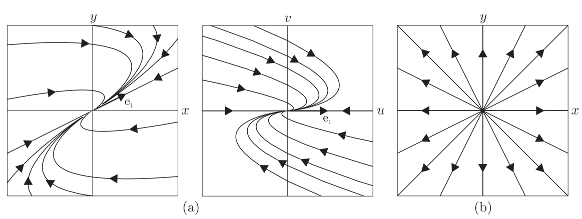

Figure 6.5. Phase portrait of linear sistem in the neighbourhood of (a) stable and (b) unstable degenerate node. [27]

7. **Source and sink:** $p^2 = 4q$, $q > 0$, $b = c = 0$ and $a = d \neq 0$. Here $dx/dt = ax$, $dy/dt = ay$. Therefore $x(t) = x_0e^{\alpha t}$ and $y(t) = y_0e^{\alpha t}$. This gives radial orbits, the origin being stable (a sink) if $a < 0$ and unstable (a source) if $a > 0$.

Note that a stable node and a stable focus are attractors and an unstable node and an unstable focus are repellers. A saddle point is neither attractor nor repeller. A centre although stable is not asymptotically stable and therefore not an attractor.

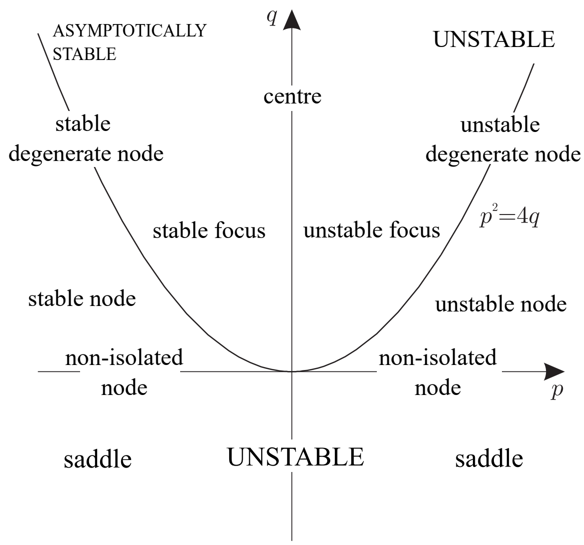

Figure 6.6. Classification of critical points in (p, q)-plane (Poincaré diagram). [27]

Bibliography

[1] David J Acheson. Elementary fluid dynamics, 1991.

[2] Martin J Canny. Applications of the compensating pressure theory of water transport. *American Journal of Botany*, 85(7):897–909, 1998.

[3] Peter Chadwick. *Continuum mechanics: concise theory and problems.* Courier Corporation, 2012.

[4] R Chebbi. Dynamics of liquid penetration into capillary tubes. *Journal of colloid and interface science*, 315(1):255–260, 2007.

[5] Hervé Cochard. Cavitation in trees. *Comptes Rendus Physique*, 7(9-10):1018–1026, 2006.

[6] Pierre Cruiziat, Hervé Cochard, and Thierry Améglio. Hydraulic architecture of trees: main concepts and results. *Annals of forest science*, 59(7):723–752, 2002.

[7] Philip G Drazin and Philip Drazin Drazin. *Nonlinear systems.* Number 10. Cambridge University Press, 1992.

[8] N Fries and M Dreyer. An analytic solution of capillary rise restrained by gravity. *Journal of colloid and interface science*, 320(1):259–263, 2008.

[9] Nicolas Fries. *Capillary transport processes in porous materials-experiment and model.* Cuvillier Verlag, 2010.

[10] Paul Glendinning. *Stability, instability and chaos: an introduction to the theory of nonlinear differential equations.* Cambridge university press, 1994.

[11] W Heber Green and GA Ampt. Studies on soil phyics. *The Journal of Agricultural Science*, 4(1):1–24, 1911.

[12] Morton E Gurtin. *An introduction to continuum mechanics.* Academic press, 1982.

[13] Morton E Gurtin, Eliot Fried, and Lallit Anand. *The mechanics and thermodynamics of continua.* Cambridge University Press, 2010.

[14] Ahmed Hamraoui and Tommy Nylander. Analytical approach for the lucas–washburn equation. *Journal of colloid and interface science*, 250(2):415–421, 2002.

[15] Dragoslav Kuzmanović, A Sedmak, I Obradović, and D Nikolić. Matematička fizika. *Rudarsko-geološki fakultet, Univerzitet u Beogradu, st*, 518, 2003.

[16] Becky Lavi, Abraham Marmur, and Joerg Bachmann. Porous media characterization by the two-liquid method: effect of dynamic contact angle and inertia. *Langmuir*, 24(5):1918–1923, 2008.

[17] Jerzy Lipiec and Inge Håkansson. Influences of degree of compactness and matric water tension on some important plant growth factors. *Soil and Tillage Research*, 53(2):87–94, 2000.

[18] Élise Lorenceau, David Quéré, Jean-Yves Ollitrault, and Christophe Clanet. Gravitational oscillations of a liquid column in a pipe. *Physics of Fluids*, 14(6):1985–1992, 2002.

[19] R Lucas. Rate of capillary ascension of liquids. *Kolloid Z*, 23(15):15–22, 1918.

[20] A Herde K Hou I Rapajić M Switala, FA Ba. Capillary moisture uptake in trees. In *First Virtual ECMI Modeling Week 2020*, 2020.

[21] Reza Masoodi and Krishna M Pillai. Traditional theories of wicking: capillary models. *Wicking in Porous Materials: Traditional and Modern Modeling Approaches*, pages 31–53, 2012.

[22] Reza Masoodi, Krishna M Pillai, and Padma Prabodh Varanasi. Role of hydraulic and capillary radii in improving the effectiveness of capillary model in wicking. In *Fluids Engineering Division Summer Meeting*, volume 48401, pages 251–259, 2008.

[23] Łukasz Płociniczak and Mateusz Świtała. Monotonicity, oscillations and stability of a solution to a nonlinear equation modelling the capillary rise. *Physica D: Nonlinear Phenomena*, 362:1–8, 2018.

[24] David Quéré, Élie Raphaël, and Jean-Yves Ollitrault. Rebounds in a capillary tube. *Langmuir*, 15(10):3679–3682, 1999.

[25] William H Schlesinger, Paul J Fonteyn, and Giles M Marion. Soil moisture content and plant transpiration in the chihuahuan desert of new mexico. *Journal of Arid Environments*, 12(2):119–126, 1987.

[26] William H Schlesinger and Scott Jasechko. Transpiration in the global water cycle. *Agricultural and Forest Meteorology*, 189:115–117, 2014.

[27] S.S. Simić. *Analitička mehanika: dinamika, stabilnost, bifurkacije*. Edicija "Tehničke nauke - udžbenici". Fakultet tehničkih nauka, 2006.

[28] Michael Stange, Michael E Dreyer, and Hans J Rath. Capillary driven flow in circular cylindrical tubes. *Physics of fluids*, 15(9):2587–2601, 2003.

[29] Ernst Steudle. The cohesion-tension mechanism and the acquisition of water by plant roots. *Annual review of plant biology*, 52(1):847–875, 2001.

[30] Lincoln Taiz, Eduardo Zeiger, Ian Max Møller, Angus Murphy, et al. *Plant physiology and development*. Number Ed. 6. Sinauer Associates Incorporated, 2015.

[31] MT Tyree, Hervé Cochard, and P Cruiziat. The water-filled versus air-filled status of vessels cut open in air: the 'scholander assumption'revisited. *Plant, Cell & Environment*, 26(4):613–621, 2003.

[32] Edward W Washburn. The dynamics of capillary flow. *Physical review*, 17(3):273, 1921.

[33] Eberhard Zeidler. *Applied functional analysis: applications to mathematical physics*, volume 108. Springer Science & Business Media, 2012.

[34] BV Zhmud, F Tiberg, and K Hallstensson. Dynamics of capillary rise. *Journal of colloid and interface science*, 228(2):263–269, 2000.

Biography

Isidora Rapajić was born on October 3, 1997 in Zrenjanin, Serbia. She received her Bachelor's degree in General Mathematics in 2019 from the Faculty of Mathematics, Natural Sciences and Information Technologies (University of Primorska, Slovenia).

The same year she enrolled in Master's programme of Applied Mathematics at the Faculty of Sciences, University of Novi Sad, Serbia. Isidora was participant of ECMI Modelling Week in July 2020 and worked on a project *"Capillary moisture uptake in wood and trees"*, which motivated this thesis.

In June 2021 she passed all exams and satisfied the requirements for specialisation in Technomathematics.

Novi Sad, 2021 Isidora Rapajić

UNIVERZITET U NOVOM SADU
PRIRODNO-MATEMATIČKI FAKULTET
KLJUČNA DOKUMENTACIJSKA INFORMACIJA

Redni broj:
RBR

Identifikacioni broj:
IBR

Tip dokumentacije: Monografska dokumentacija
TD

Tip zapisa: Tekstualni štampani materija
TZ

Vrsta rada: Master rad
VR

Autor: Isidora Rapajić
AU

Mentor: dr Srboljub Simić
MN

Naslov rada: Modeliranje kapilarnih pojava u biljnom vaskularnom tkivu
NR

Jezik publikacije: engleski
JP

Jezik izvoda: srpski/engleski
JI

Zemlja publikovanja: Republika Srbija
ZP

Uže geografsko područje: Vojvodina
UGP

Godina: 2021.
GO

Izdavač: Autorski reprint
IZ

Mesto i adresa: Univerzitet u Novom Sadu, Prirodno-matematički fakultet, Trg Dositeja Obradovića

4
MA

Fizički opis rada: (5/63/34/0/14/8/1)
(broj poglavlja/strana/lit citata/tabela/slika/grafika/priloga)
FO

Naučna oblast: Matematika
NO

Naučna disciplina: Matematičko modeliranje
ND

Predmetna odrednica/Ključne reči: Biljno vaskularno tkivo, Vošburnova jednačina, Zakoni održanja, Egzistencija i jedinstvenost, Košijeva teorema, Analiza stabilnosti, Asimptotska analiza
PO

UDK

Čuva se: u biblioteci Departmana za matematiku i informatiku, Novi Sad
CU

Važna napomena:
VN

Izvod: Predmet ovog rada je formulisanje matematičkog modela za kapilarni uspon u biljnom vaskularnom tkivu. Cilj je izvodjenje i skaliranje glavne jednačine a zatim asimptotska analiza i analiza stabilnosti. U prvom poglavlju date su osnove fiziologije biljaka neophodne za postavljanje modela. Biljno provodno tkivo se modeluje cilindričnom cevi. Drugo poglavlje je posvećeno izvodjenju Vošburnove jednačine iz zakona održanja u mehanici neprekidnih sredina i izvršeno je njeno skaliranje. U trećem poglavlju daje se dokaz egzistencije i jedinstvenosti rešenja. Dalje, pokazano je da je rešenje uvek pozitivno i odredjene su granice rešenja. U četvrtom poglavlju su izvedene asimptotska analiza i analiza stabilnosti. Odreena je kritična vrednost bezdimenzijskog parametra pri kojoj dolazi do promene karaktera rešenja. Ovo je potvrdjeno numeričkim rešavanjem jednačine i prikazivanjem faznih portreta. Rešenje jednačine je poreeno sa eksperimentalnim rezultatima u početnom režimu uspona i pokazano je dobro slaganje.
IZ

Datum prihvatanja teme od strane NN veća: 22.06.2021.
DP

Datum odbrane:
DO

Članovi komisije:
KO

Predsednik: dr Danijela Rajter Ćirić, redovni profesor, Prirodno-matematički fakultet, Univerzitet u Novom Sadu

Član: dr Mirjana Štrboja, vanredni profesor, Prirodno-matematički fakultet, Univerzitet u Novom Sadu

Član: dr Milan Borišev, redovni profesor, Prirodno-matematički fakultet, Univerzitet u Novom Sadu

Mentor: dr Srboljub Simić, redovni profesor, Prirodno-matematički fakultet, Univerzitet u Novom Sadu

UNIVERSITY OF NOVI SAD
FACULTY OF SCIENCES
KEY WORDS DOCUMENTATION

Accession number:
ANO

Identification number:
INO

Document type: Monograph type
DT

Type of record: Printed text
TR

Contents Code: Master's thesis
CC

Author: Isidora Rapajić
AU

Mentor: Srboljub Simić, Ph.D.
MN

Title: Modelling Capillary Rise In The Vascular Tissue Of Plants
TI

Language of text: English
LT

Language of abstract: Serbian/English
LA

Country of publication: Serbia
CP

Locality of publication: Vojvodina
LP

Publication year: 2017.
PY

Publ. place: Novi Sad, Department of Mathematics and Informatics, Faculty of Science and Mathematics, University of Novi Sad, Trg Dositeja Obradovića 4
PP

Physical description: (5/63/34/0/14/8/1)
(number of sections/pages/references/tables/pictures/graphs/appendices)
PD

Scientific field: Mathematics
SF

Scientific discipline: Mathematical modelling
SD

Subject/Key words: Vascular tissue of plants, Washburn's equation, Balance laws, Existence and uniqueness, Cauchy's Fixed Point Theorem, Stability analysis, Asymptotic analysis
SKW

UC:

Holding data: The Library of the Department of Mathematics and Informatics, Faculty of Science and Mathematics, University of Novi Sad
HD

Note:
N

Abstract: The subject of this thesis is to analyse the mathematical aspects of capillary rise in the vascular tissue of plants. The goal is to derive and scale the governing equation of capillary rise and then to conduct stability and asymptotic analysis. A building block of plants' vascular tissue is modelled as a cylindrical pipe. Chapter 1 contains biological explanation of the phenomena. Chapter 2 is dedicated to derivation of Washburn's equation using the fundamental equations from continuum mechanics. Additionally, scaling of the governing equation and initial conditions are provided. In Chapter 3, the goal was to prove existence and uniqueness of a solution. Moreover, it is shown that the solution is always positive, and bounds of the solution are determined. Finally, Chapter 4 contains asymptotic and stability analysis. Stationary point is determined and it is shown that the stationary state can be either monotonically or oscillatory approached, which is verified by numerical analysis. Real experimental data is compared with our model and results are observed to be in a good agreement.
AB

Accepted by the Scientific Board on: 22.06.2021
ASB

Defended:
DE

Thesis defend board:
DB

President: Danijela Rajter Ćirić, PhD, full professor, Faculty of Sciences, University of Novi Sad

Member: Mirjana Štrboja, PhD, associate professor, Faculty of Sciences, University of Novi Sad

Member: Milan Borišev, PhD, full professor, Faculty of Sciences, University of Novi Sad

Mentor: Srboljub Simić, PhD, full professor, Faculty of Sciences, University of Novi Sad